Data-Driven Methods for Image Reconstruction and Artifact Correction in CBCT

Marc Kachelrieß

German Cancer Research Center (DKFZ)

Heidelberg, Germany

www.dkfz.de/ct

DEUTSCHES KREBSFORSCHUNGSZENTRUM IN DER HELMHOLTZ-GEMEINSCHAFT

Outline

- Sparse view
- Ring artifacts
- Metal artifacts
- Scatter estimation
- Motion compensation
- 3D fluoroscopy (3D + time)

Sparse View Restoration Example

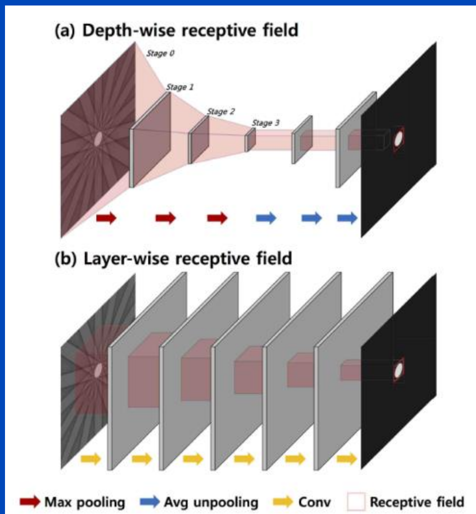

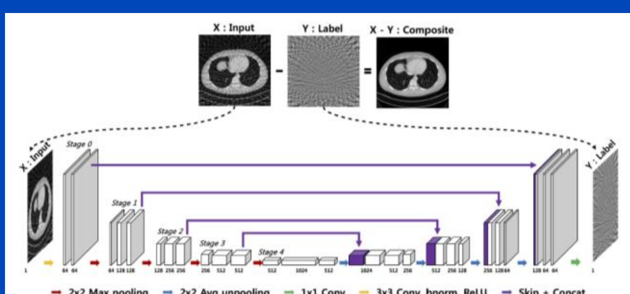

Figure 1. The proposed deep residual learning architecture for sparse view CT reconstruction.

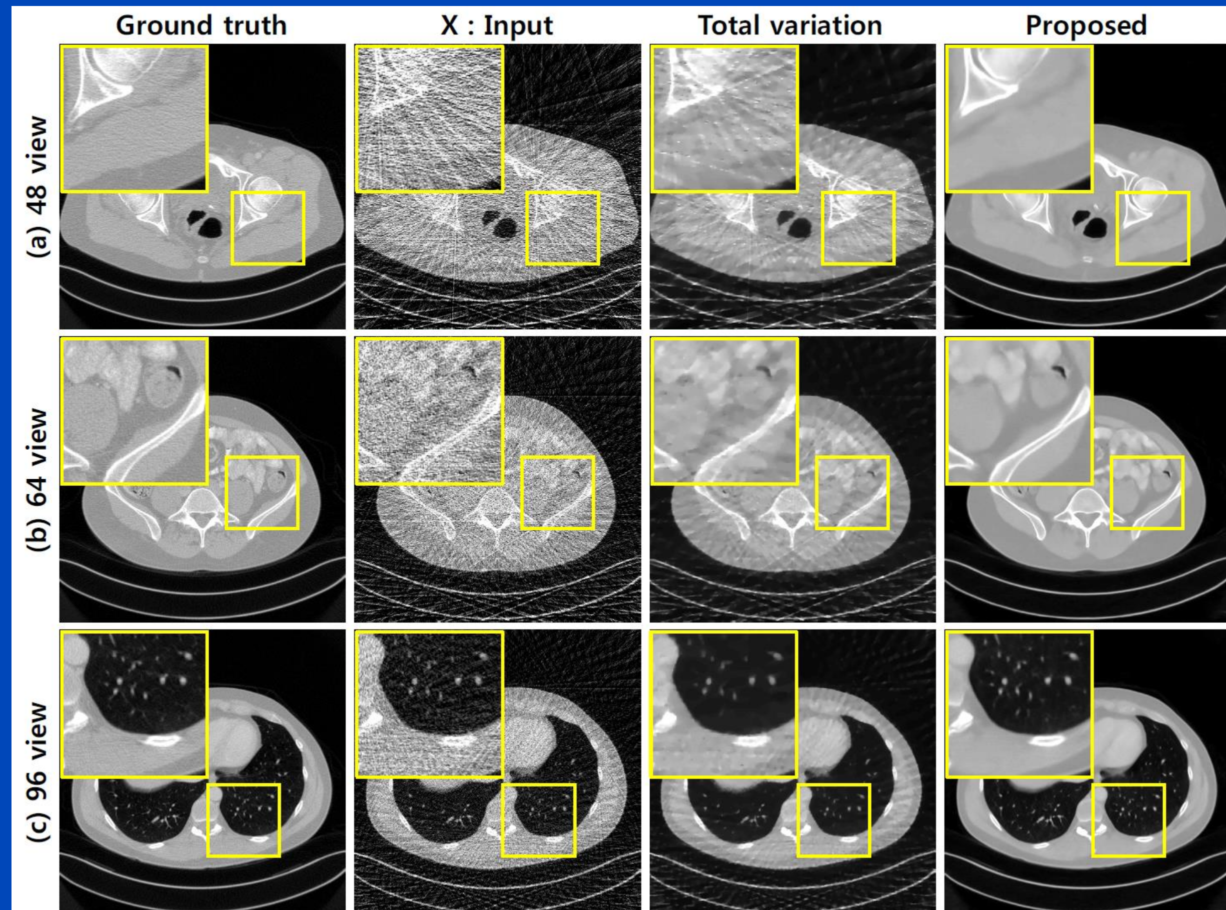

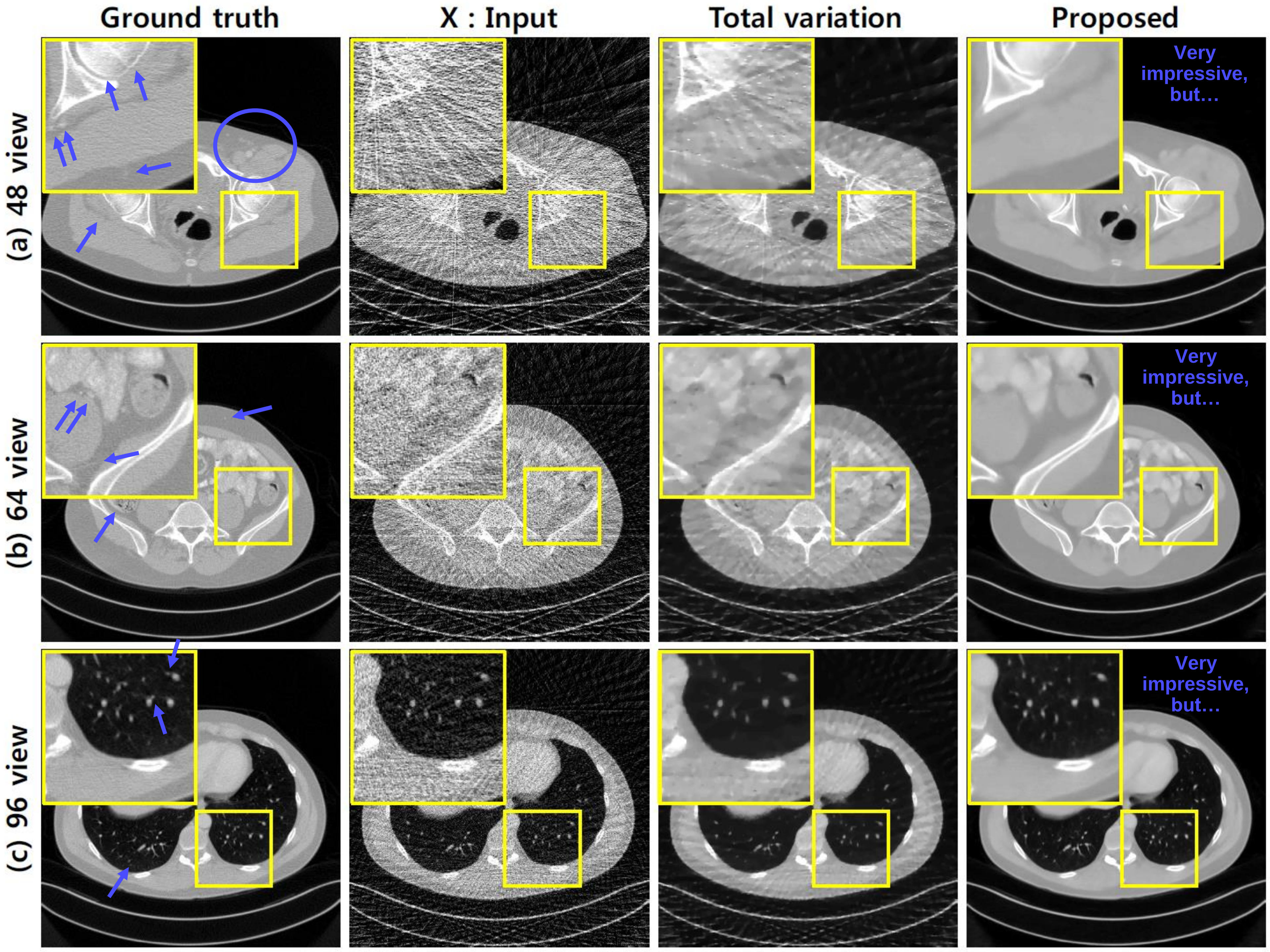

Ground truth
X : Input
Total variation
Proposed
(a) 48 view
(b) 64 view
(c) 96 view
Very impressive, but…
Very impressive, but…
Very impressive, but…

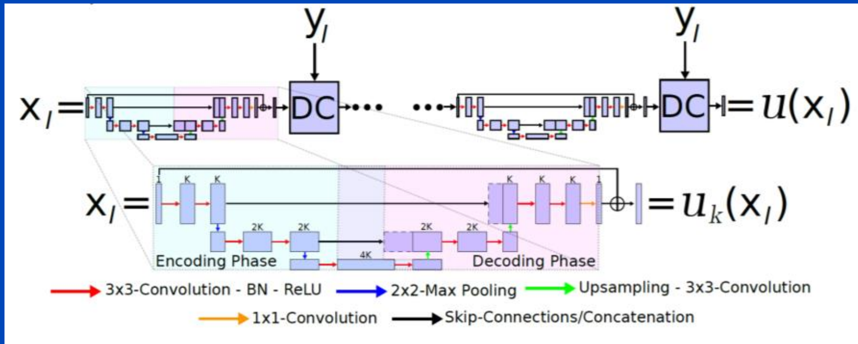

Sparse CT Recon with Data Consistency Layers (DCLs)

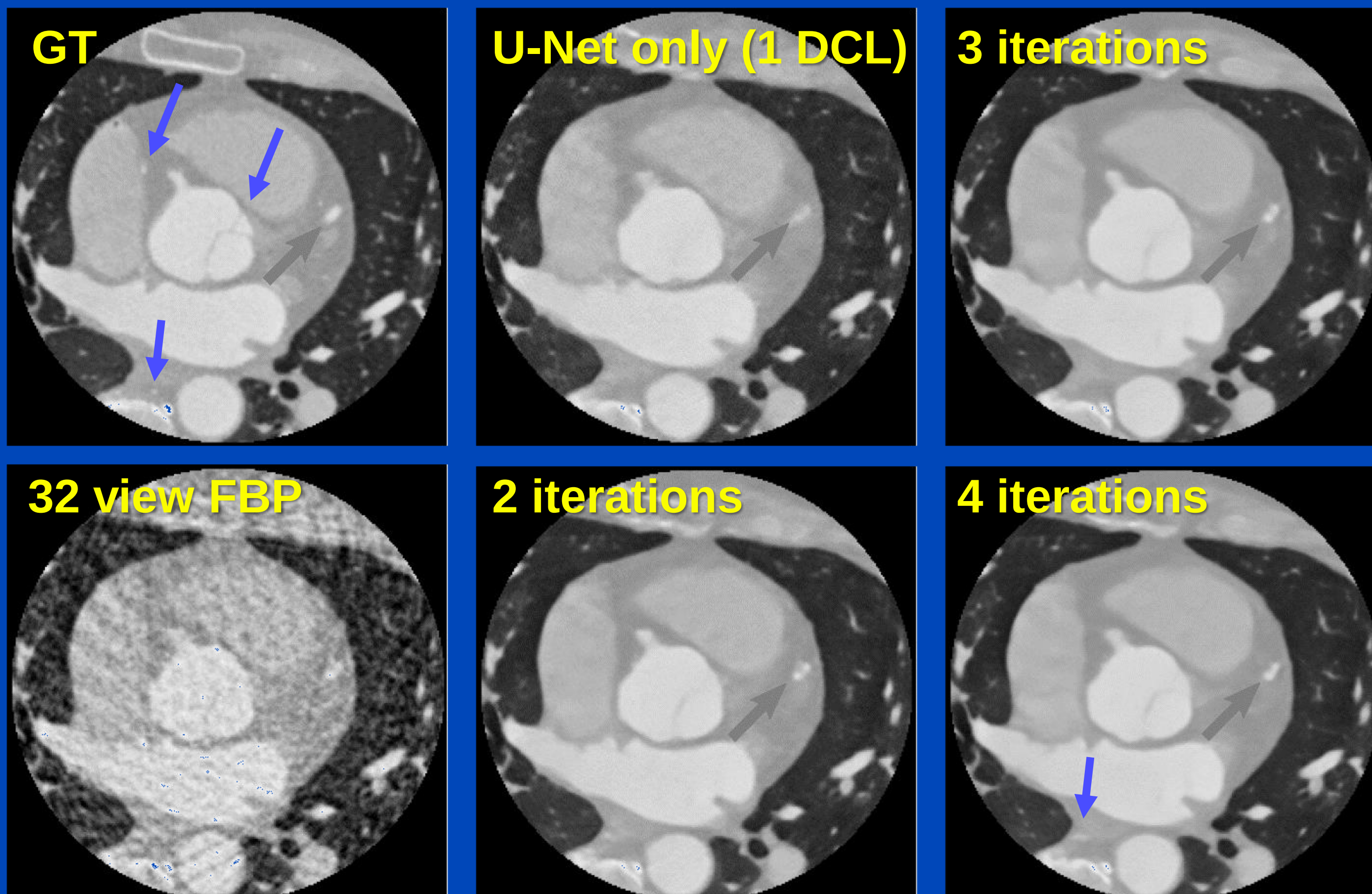

A. Kofler, M. Haltmeier, C. Kolbitsch, M. Kachelrieß, and M. Dewey. A U-Nets Cascade for Sparse View Computed Tomography, MICCAI 2018

Ring Artifact Reduction: Literature

- **Correction in sinogram/rawdata domain:**
  - **Nauwynck et al., *Ring Artifact Reduction in Sinogram Space Using Deep Learning*, Proc. CT Meeting 2020:486–489, 2020**
- **Correction in image domain:**
  - **Chang et al ., *A Hybrid Ring Artifact Reduction Algorithm Based on CNN in CT Images*, Fully 3D 11072:1107226, 2019**
  - **Chao et al., *Removal of Computed Tomography Ring Artifacts via Radial Basis Function Artificial Neural Networks*, Phys. Med. Biol. 64(23):235015, 2019**
  - **Kornilov et al., *Deep Neural Networks for Ring Artifacts Segmentation and Corrections in Fragments of CT Images*, 28th FRUCT conference:181-193, 2021**
  - **Wang et al., *Removing Ring Artifacts in CBCT via GAN with Unidirectional Relative Total Variation Loss*, Neural Computing and Applications 31(9):5147-5158, 2019**
  - **Lv et al., *Image Denoising and Ring Artifacts Removal for Spectral CT via Deep Neural Network*, IEEE Access 8:225594-225601, 2020**
- **Correction in both, sinogram/raw-data and image domain:**
  - **Fang et al., *Comparison of Ring Artifacts Removal by Using Neural Network in Different Domains*, MIC, 2019**
  - **Fang et al., *Removing Ring Artefacts for Photon-Counting Detectors Using Neural Networks in Different Domains*, IEEE Access 8:42447-42457, 2020**

Ring Artifact Reduction: Comments

- **Correction in sinogram/rawdata domain:**
  - **Nauwynck et al. (2020) – Results are ok. The method can, however, not correct low-frequency ring artifacts.**
- **Correction in image domain:**
  - **Chang et al. (2019) – Strange mixture of CNN and classical method. New artifacts are introduced.**
  - **Chao et al. (2019) – It remains unclear how the artifact areas are segmented. Only zoom-ins show some improvements.**
  - **Kornilov et al. (2021) – Theoretically sound, however, no reasonable images are presented.**
  - **Wang et al. (2019) – The results of all correction methods look the same (suboptimal gray scale windowing).**
  - **Lv et al. (2020) – The question arises why the method to generate the ground-truth data is not directly used for correction.**
- **Correction in both, sinogram/raw-data and image domain:**
  - **Fang et al. (2019) – The results shown are interesting. However, there are no measuremed data processed.**
  - **Fang et al. (2020) – The results are good. Probably it is the best method of this slide's list.**

Removing Ring Artefacts for Photon-Counting Detectors Using Neural Networks in Different Domains

WEI FANG, LIANG LI, (Senior Member, IEEE), AND ZHIQIANG CHEN

- Clean data from the AAPM Low Dose CT Grand Challenge.
- Ring artifacts are simulated by adding stripes in the sinogram data.
  - Slope and offset model in log domain
- The data were split into training (4800 images), validation (600 images) and testing datasets (526 images) and an MSE loss function is used.
- Simulate ring artifacts
  - slope and offset model in log domain

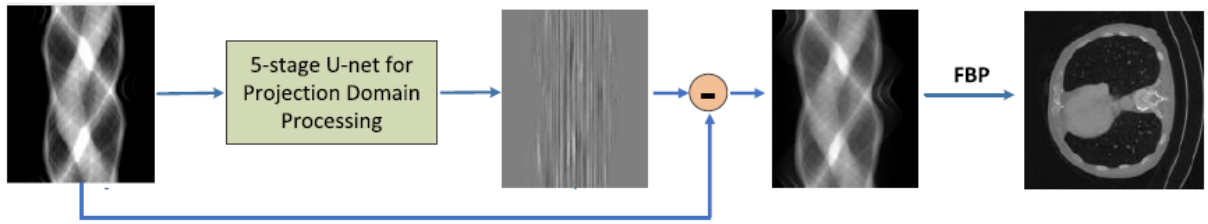

FIGURE 3. The diagram of ring artefacts removal in projection domain.

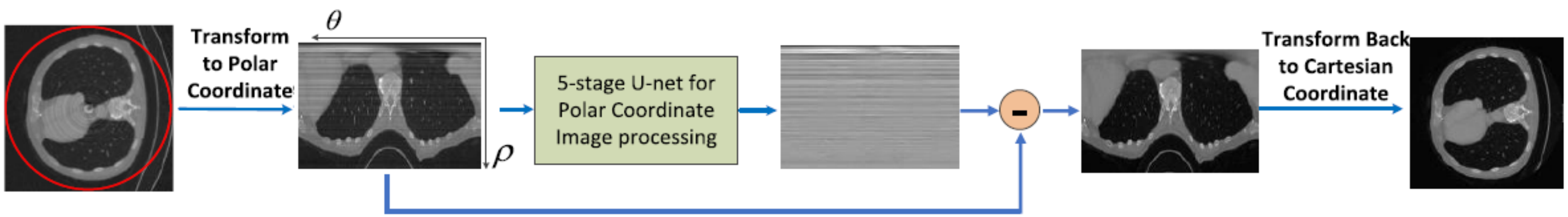

FIGURE 4. The diagram of ring artefacts removal in polar coordinate system.

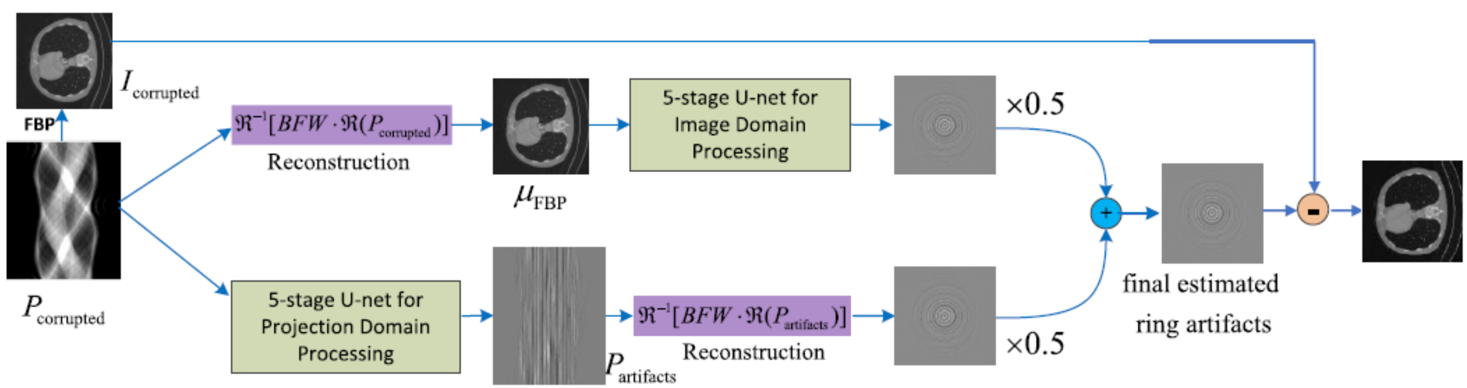

FIGURE 5. The diagram of ring artefacts removal using a comprehensive model.

Fang, Li, and Chen. Removing Ring Artefacts for Photon-Counting Detectors Using Neural Networks in Different Domains. IEEE Access 8:42447-42457, 2020.

Wavelet projection domain

Wavelet polar image domain

U-net image domain

U-net projection domain

U-net polar image domain

U-net in both domains

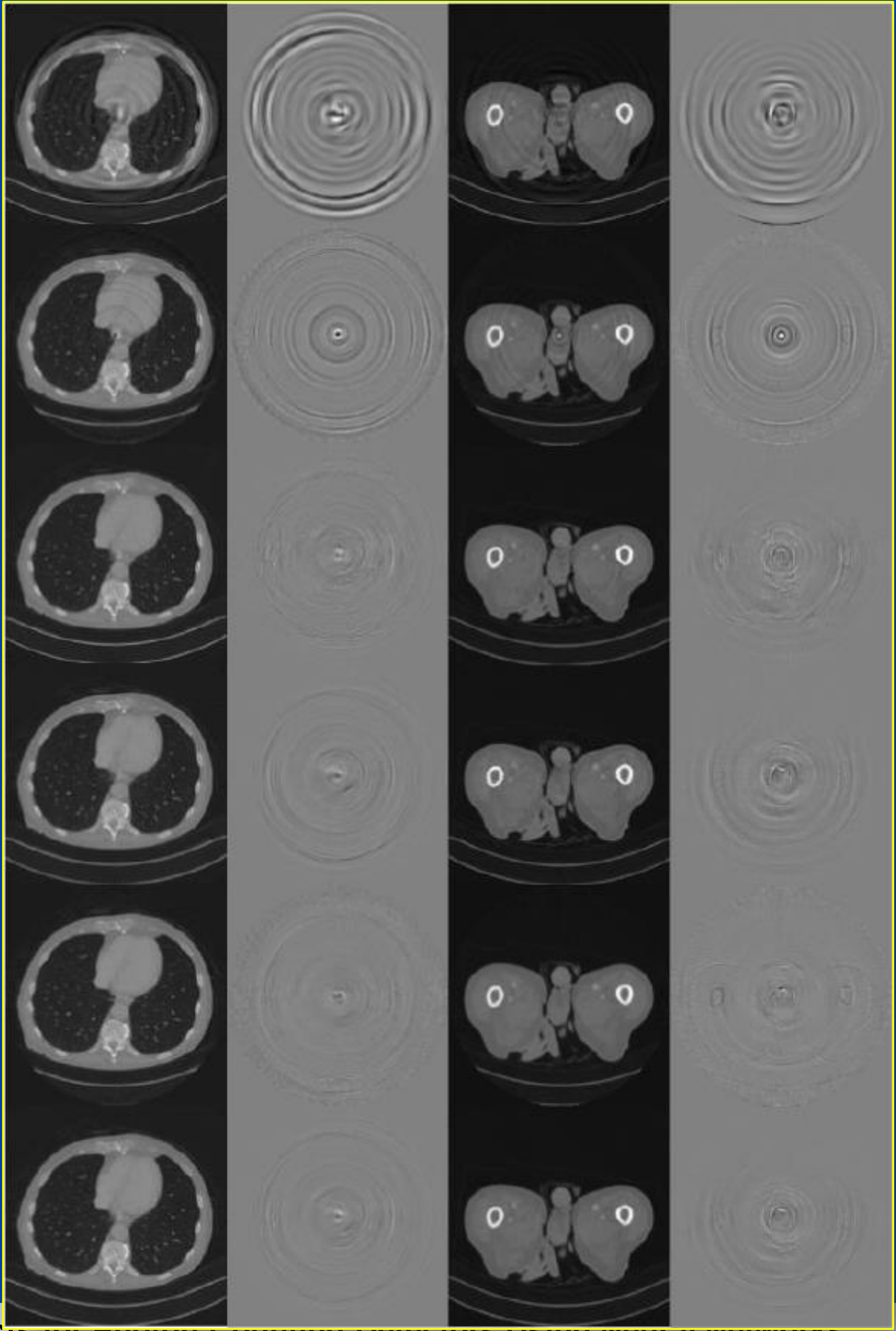

Fang, Li, and Chen. Removing Ring Artefacts for Photon-Counting Detectors Using Neural Networks in Different Domains. IEEE Access 8:42447-42457, 2020.

MAR Examples

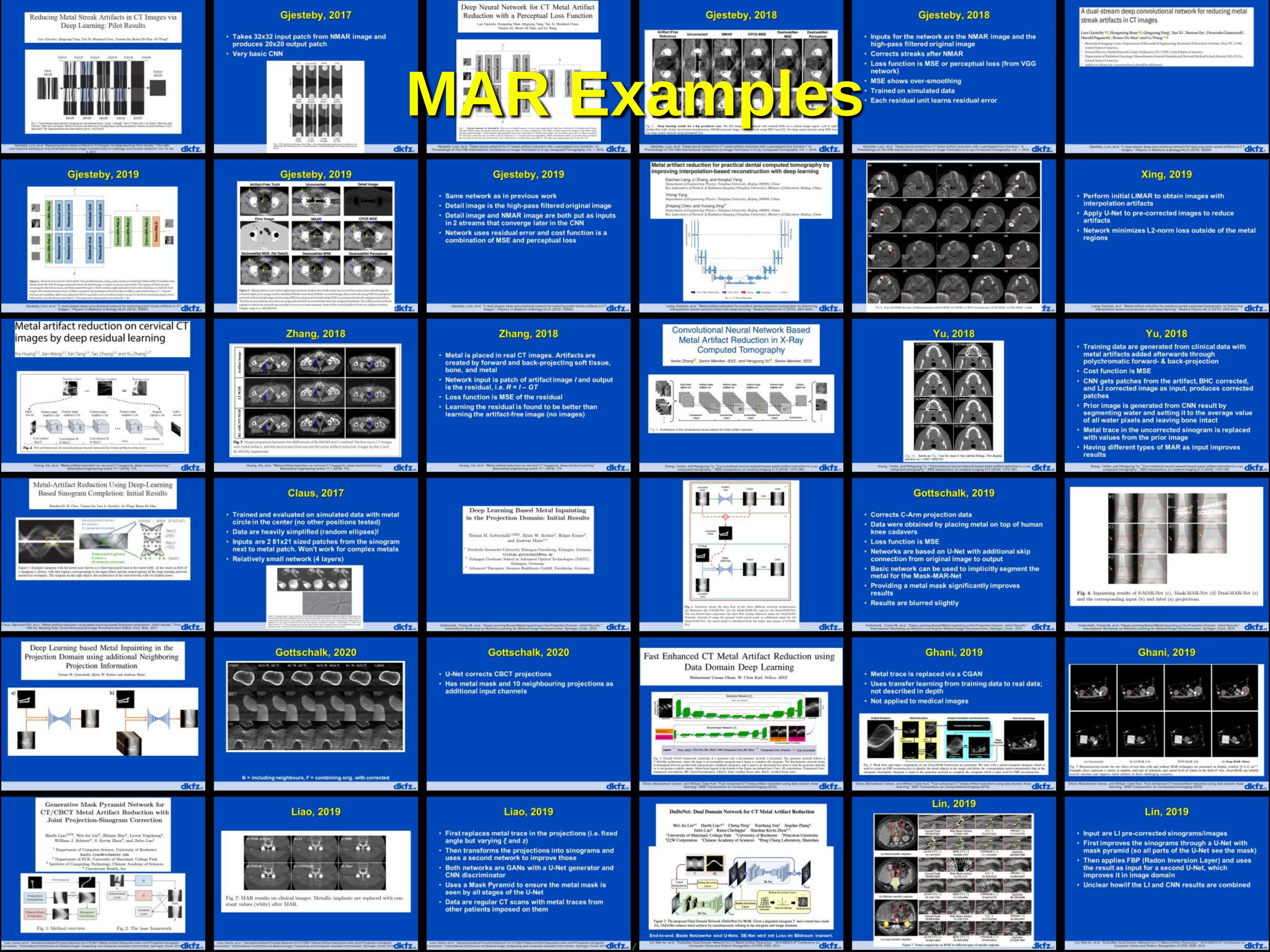

MAR Example

- Deep CNN-driven patch-based combination of the advantages of several MAR methods trained on simulated artifacts

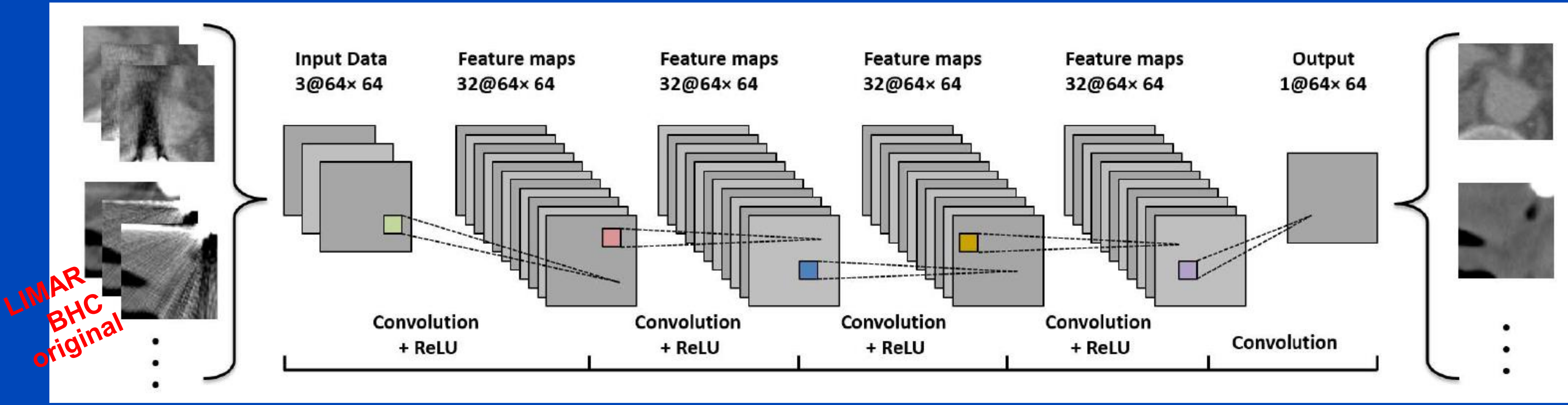

- followed by segmentation into tissue classes
- followed by forward projection of the CNN prior and replacement of metal areas of the original sinogram
- followed by reconstruction

Yanbo Zhang and Hengyong Yu. Convolutional Neural Network Based Metal Artifact Reduction in X-Ray Computed Tomography. TMI 37(6):1370-1381, June 2018.

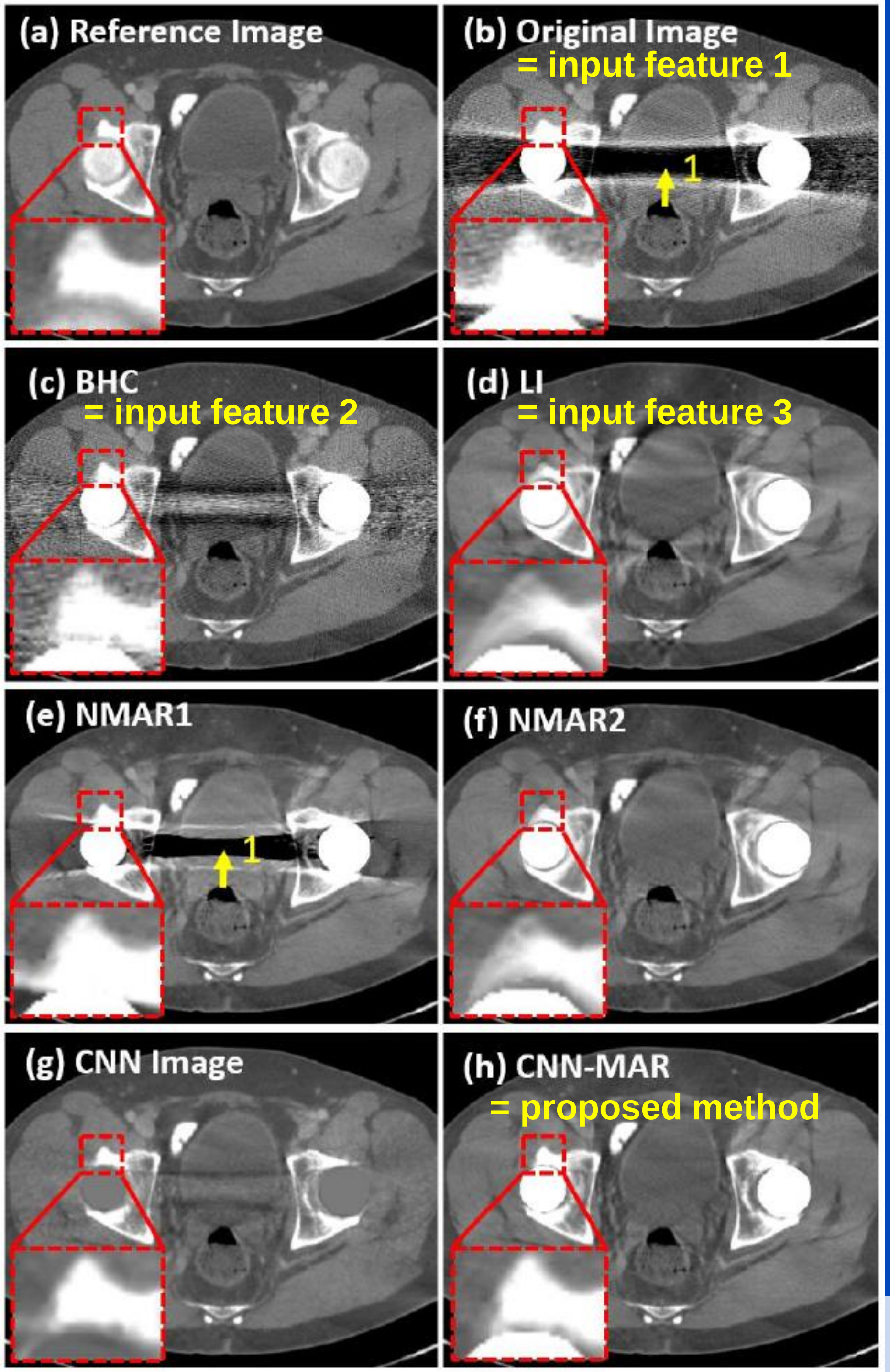
(a) Reference Image
(b) Original Image
= input feature 1
1
(c) BHC
= input feature 2
(d) LI
= input feature 3
(e) NMAR1
1
(f) NMAR2
(g) CNN Image
(h) CNN-MAR
= proposed method

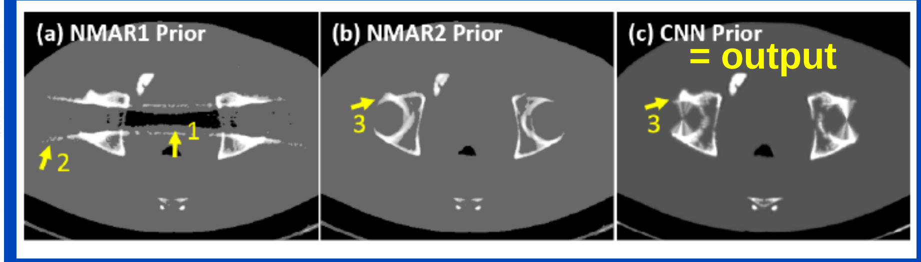
(a) NMAR1 Prior
2
1
(b) NMAR2 Prior
3
(c) CNN Prior
= output
3

dkfz.

Deep Scatter Estimation

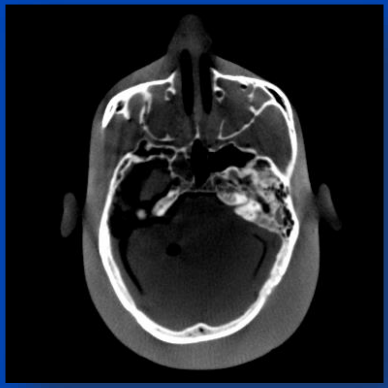

???

In real time?

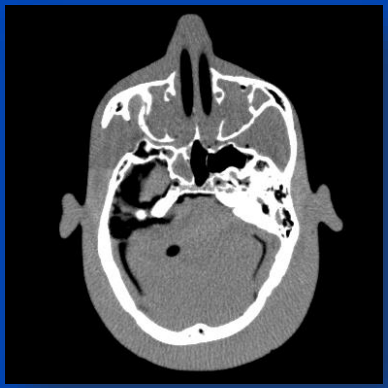

Monte Carlo Scatter Estimation

- Simulation of photon trajectories according to physical interaction probabilities.
- Simulating a large numb… …ries well approximat…

1 to 10 hours per tomographic data set

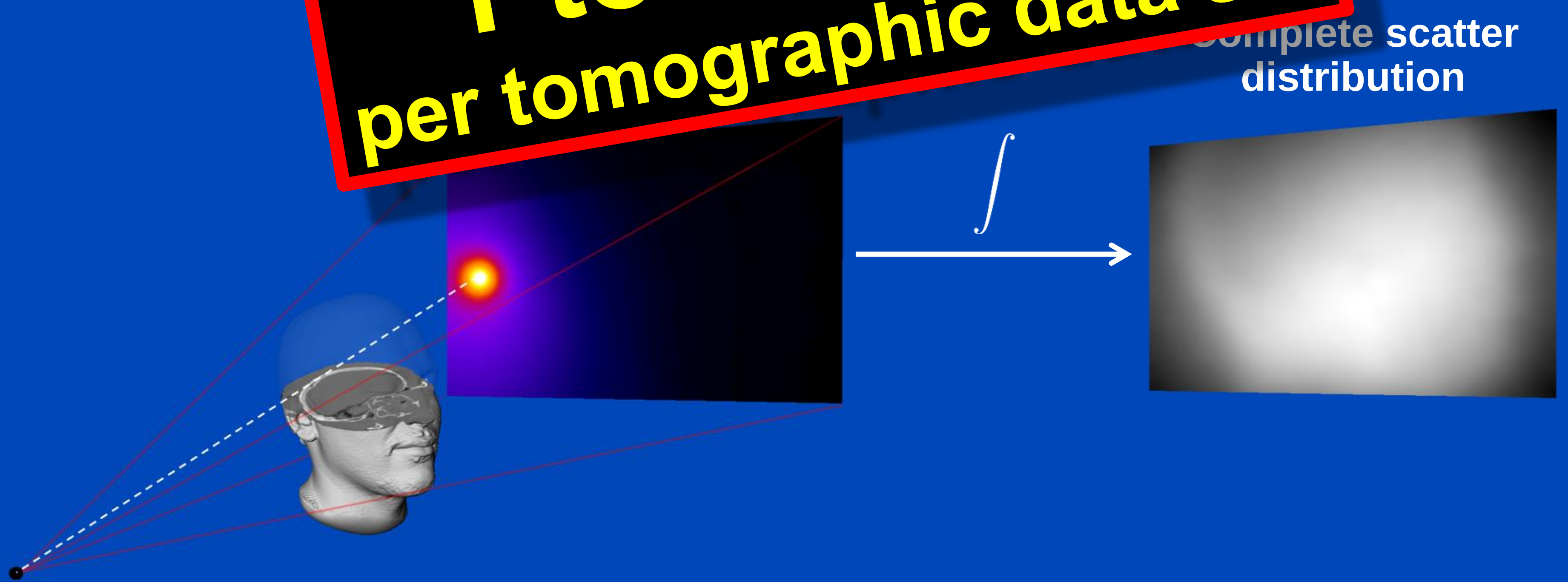

Deep Scatter Estimation

Network architecture & scatter estimation framework

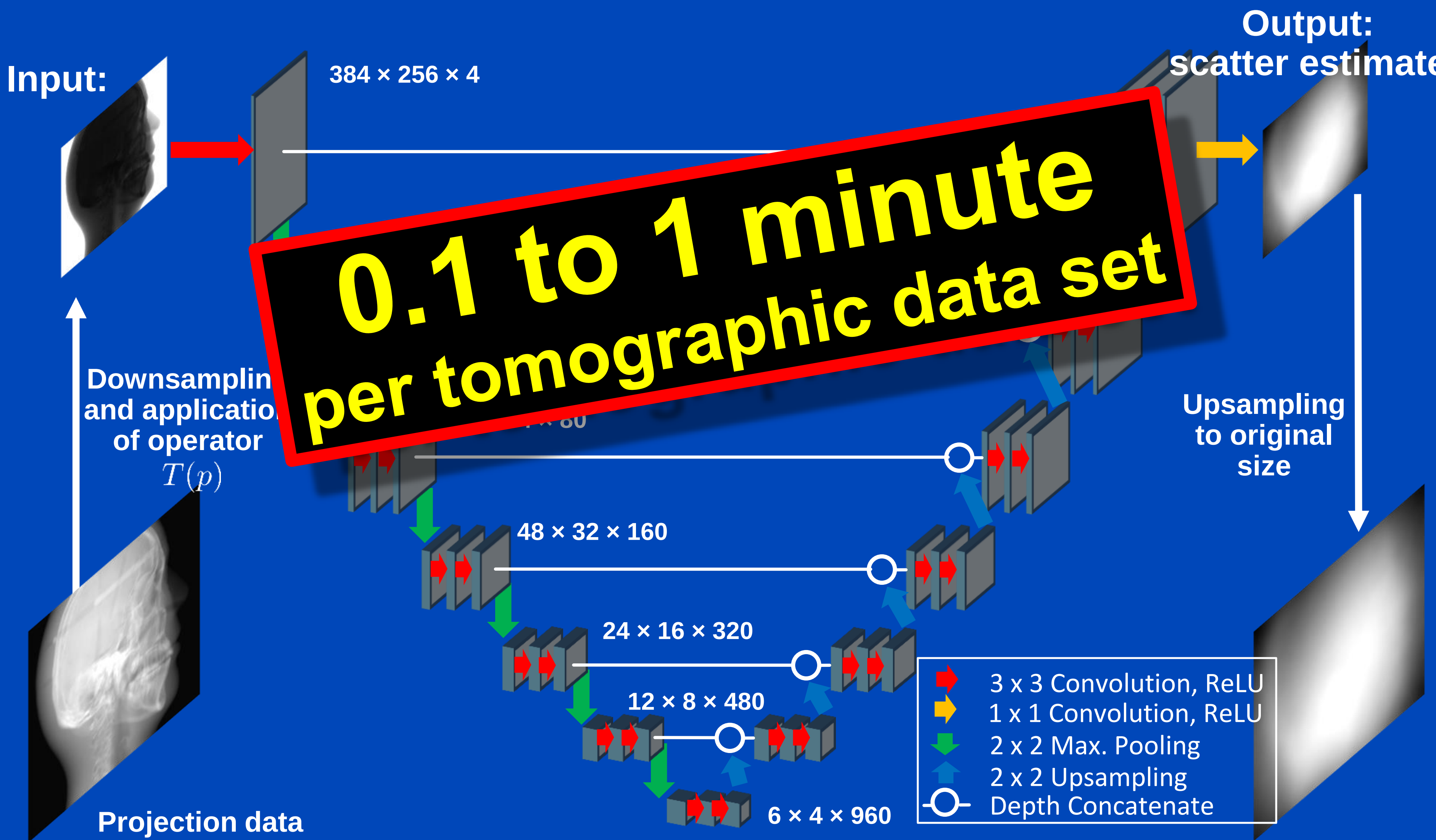

J. Maier, M. Kachelrieß et al. Deep scatter estimation (DSE). SPIE 2017 and Journal of Nondestructive Evaluation 37:57, July 2018.
J. Maier, M. Kachelrieß et al. Robustness of DSE. Med. Phys. 46(1):238-249, January 2019.

Results on Simulated Projection Data

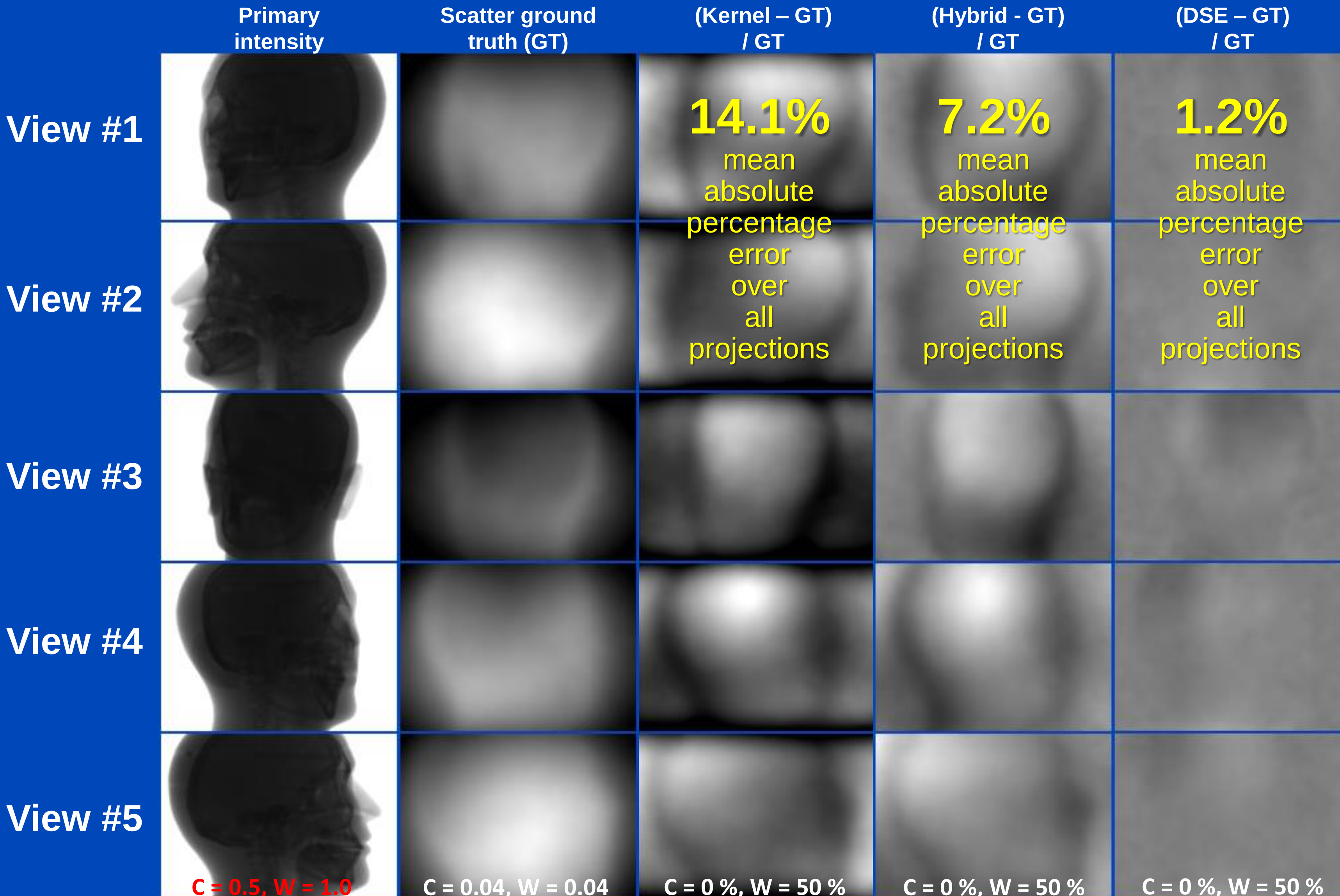

DSE trained to estimate scatter from **primary plus scatter**: High accuracy

Reconstructions of Simulated Data

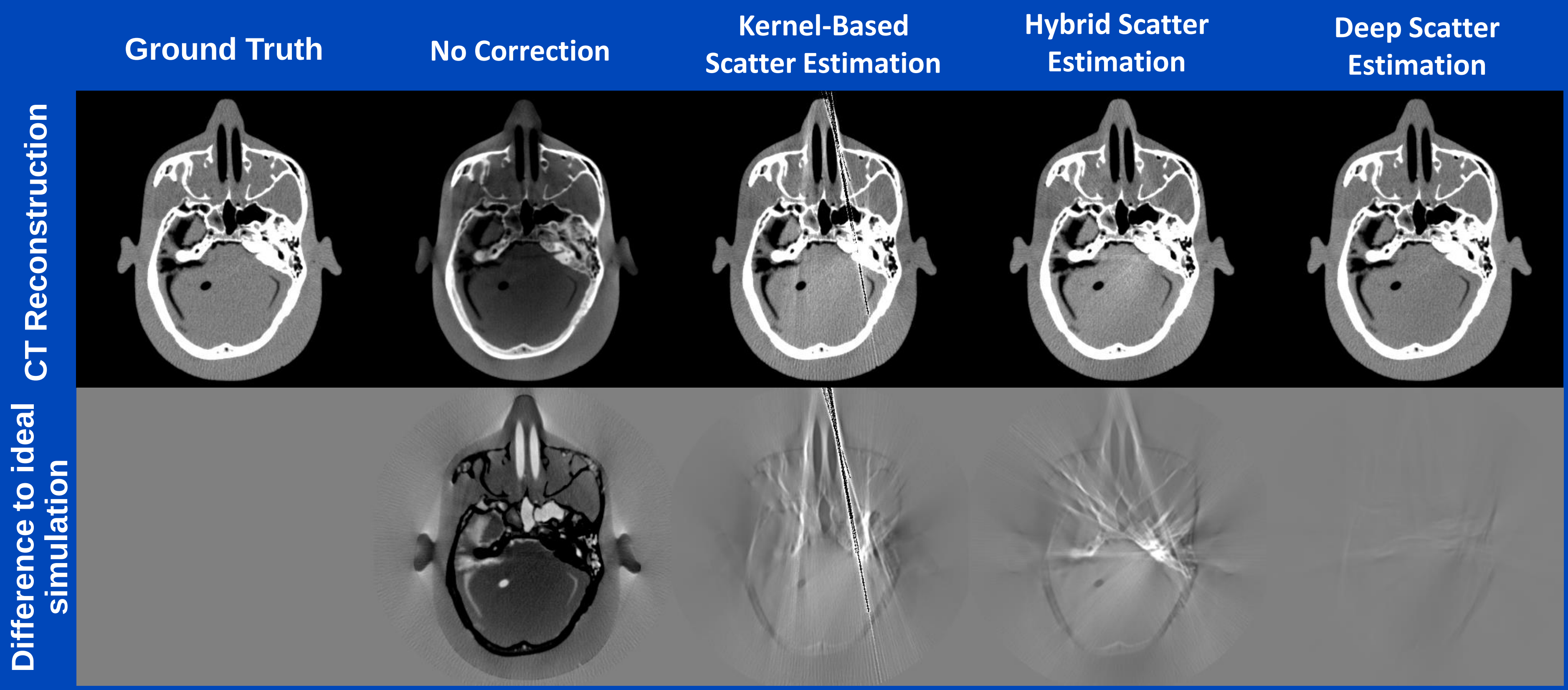

C = 0 HU, W = 1000 HU

J. Maier, M. Kachelrieß et al. Deep scatter estimation (DSE). SPIE 2017 and Journal of Nondestructive Evaluation 37:57, July 2018.
J. Maier, M. Kachelrieß et al. Robustness of DSE. Med. Phys. 46(1):238-249, January 2019.

Testing of the DSE Network for Measured Data (120 kV)

DKFZ table-top CT

- Measurement of a head phantom at our in-house table-top CT.
- Slit scan measurement serves as ground truth.

Measurement to be corrected

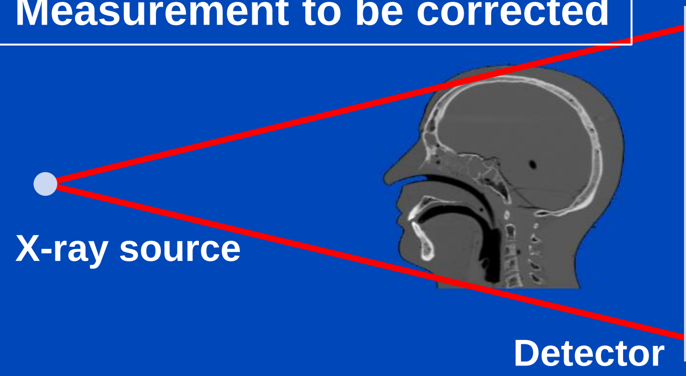

Ground truth: slit scan

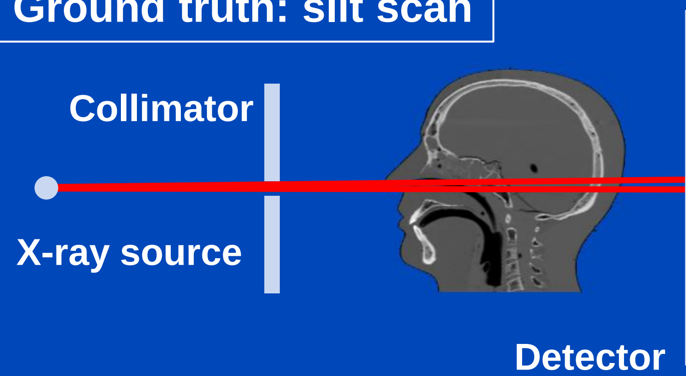

J. Maier, M. Kachelrieß et al. Deep scatter estimation (DSE). SPIE 2017 and Journal of Nondestructive Evaluation 37:57, July 2018.
J. Maier, M. Kachelrieß et al. Robustness of DSE. Med. Phys. 46(1):238-249, January 2019.

Reconstructions of Measured Data

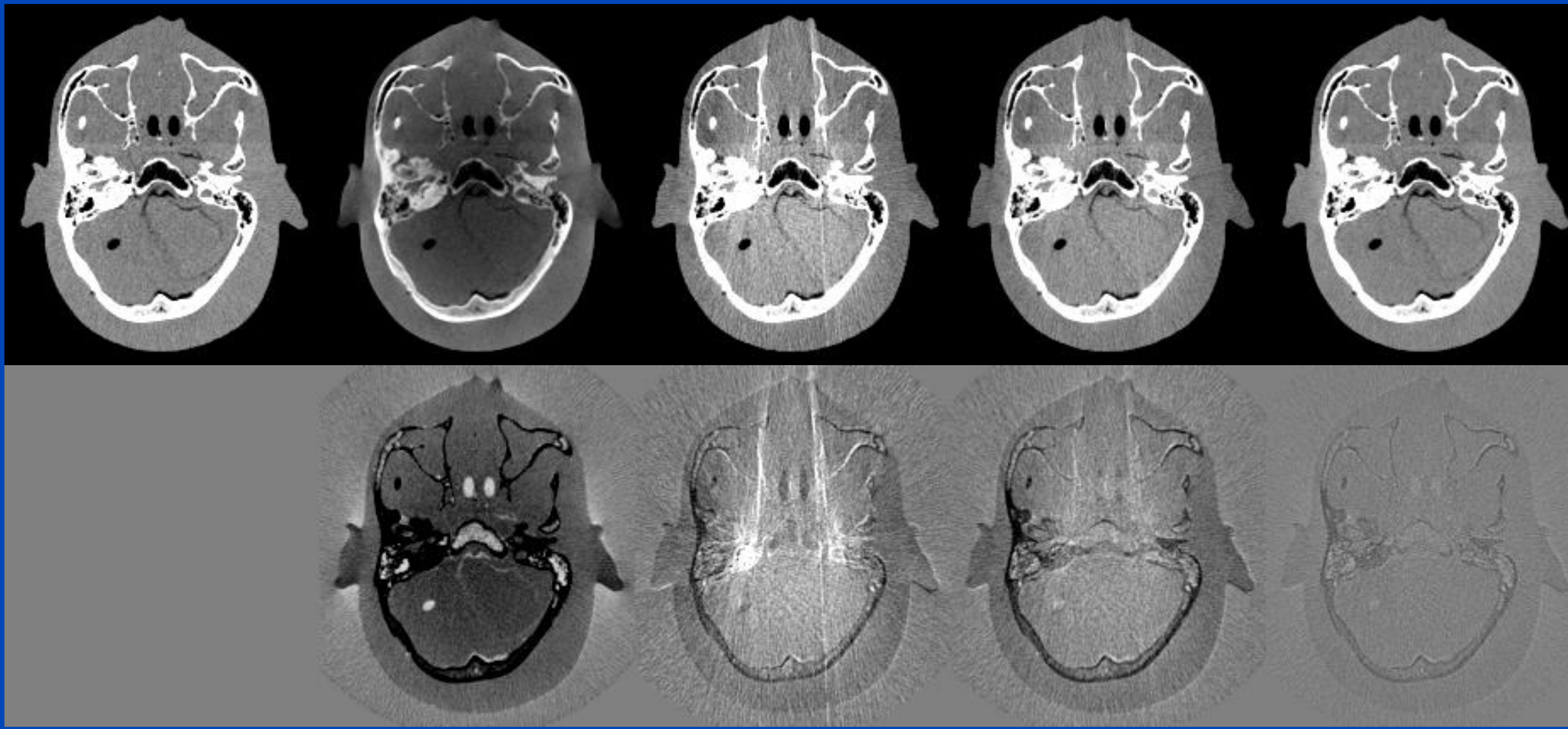

C = 0 HU, *W* = 1000 HU

J. Maier, M. Kachelrieß et al. Deep scatter estimation (DSE). SPIE 2017 and Journal of Nondestructive Evaluation 37:57, July 2018.
J. Maier, M. Kachelrieß et al. Robustness of DSE. Med. Phys. 46(1):238-249, January 2019.

Conclusions on DSE

- DSE needs about 3 ms per CT and 10 ms per CBCT projection (as of 2020).
- DSE is a fast and accurate alternative to MC simulations.
- DSE outperforms kernel-based approaches in terms of accuracy and speed.
- Facts:
  - DSE can estimate scatter from a single (!) x-ray image.
  - DSE can accurately estimate scatter from a primary+scatter image.
  - DSE generalizes to all anatomical regions.
  - DSE works for geometries and beam qualities differing from training.
  - DSE may outperform MC even though DSE is trained with MC.
- DSE is not restricted to reproducing MC scatter estimates.
- DSE can rather be trained with any other scatter estimate, including those based on measurements.

Deep Cardiac Motion Compensation

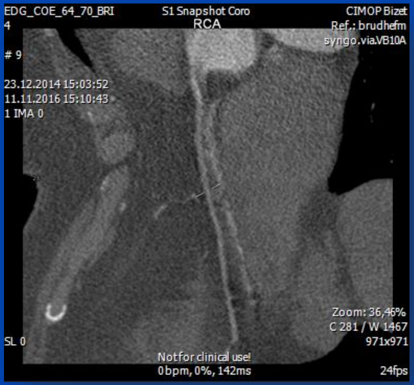

???

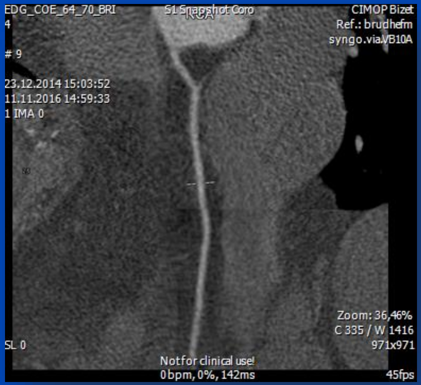

dkfz.

Deep PAMoCo

Network architecture

Initial volume
(with motion artifacts)

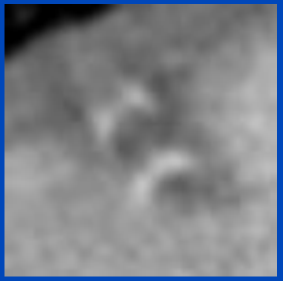

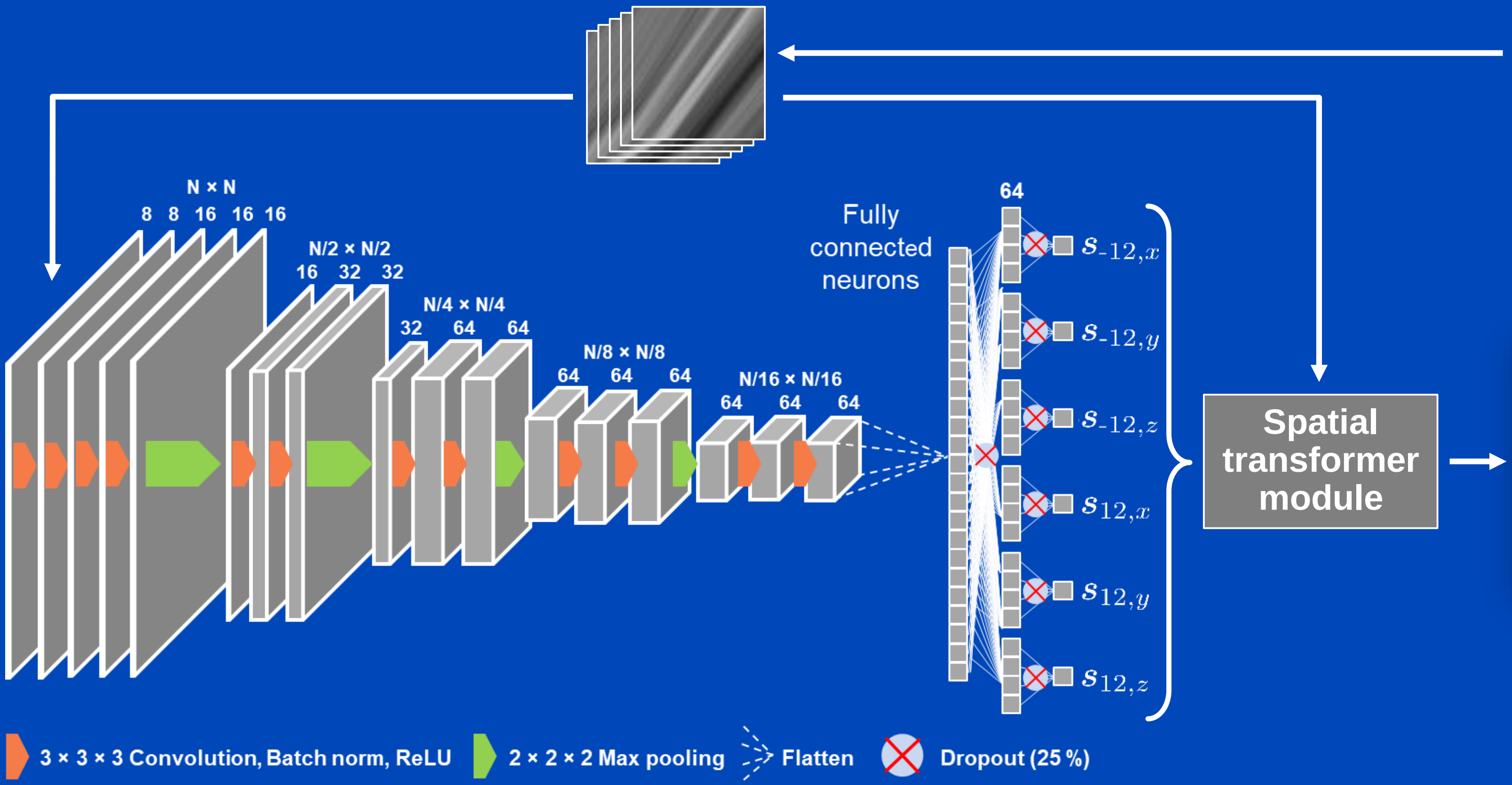

Final volume
(no motion artifacts)

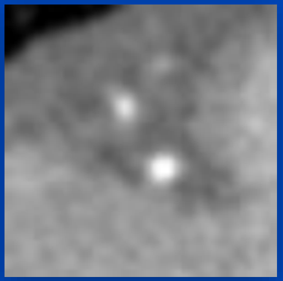

FCN-Layer output: two control points for a cubic spline: for *k* = –*K*, and for *k* = +*K*. The third control point at *k* = 0 is (0, 0, 0), i.e. no deformation for the central PAR.

J. Maier, S. Lebedev, J. Erath, E. Eulig, S. Sawall, E. Fournié, K. Stierstorfer, M. Lell, and M. Kachelrieß. Deep learning-based coronary artery motion estimation and compensation for short-scan cardiac CT. Med. Phys. 48, in press, 2021.

Results

Measurements, patient 1

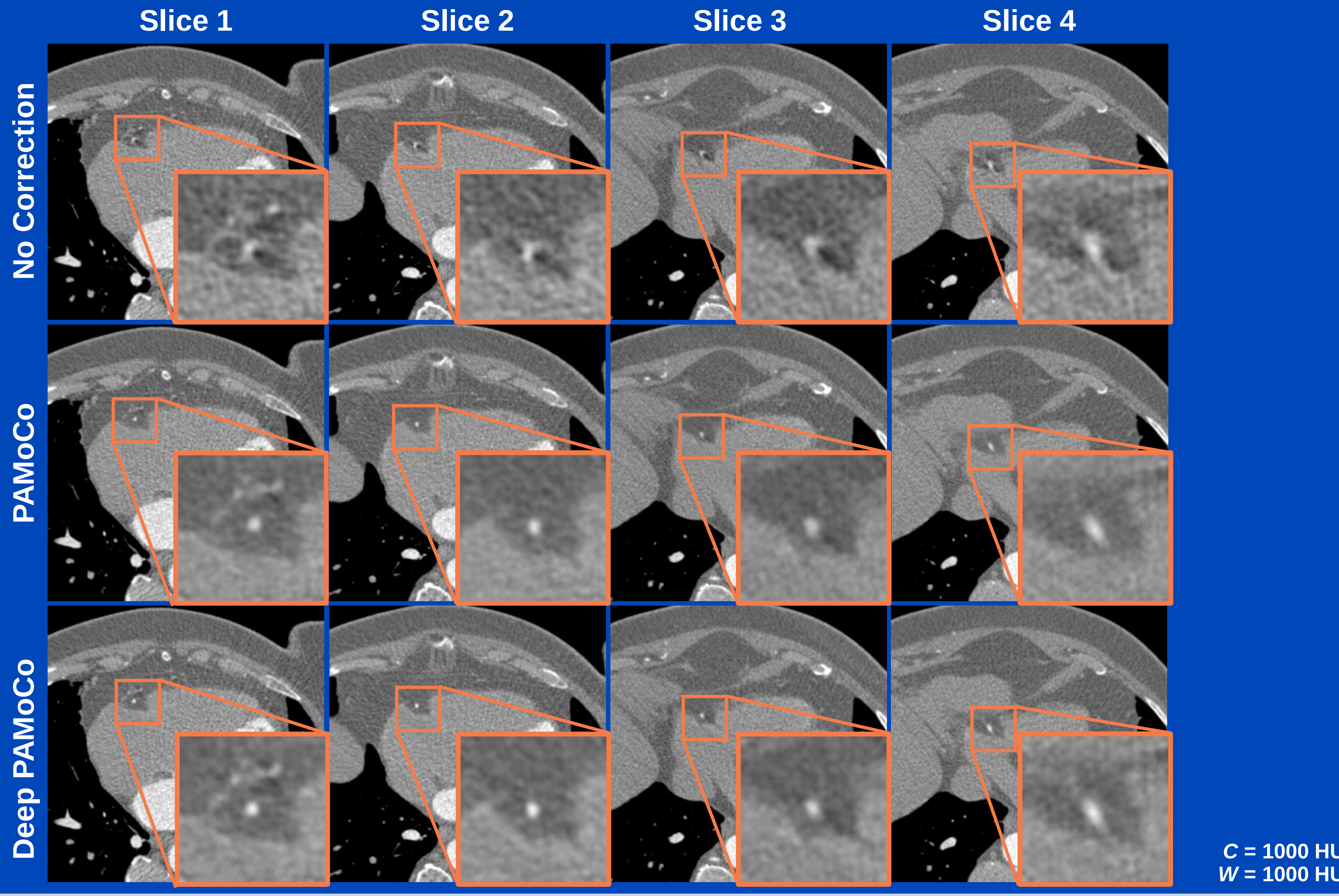

J. Maier, S. Lebedev, E. Eulig, S. Sawall, E. Fournié, K. Stierstorfer, and M. Kachelrieß. Coronary artery motion compensation for short-scan cardiac CT using a spatial transformer network. Conference Program of the 6th International CT-Meeting, August 2020.

Results

Measurements, patient 2

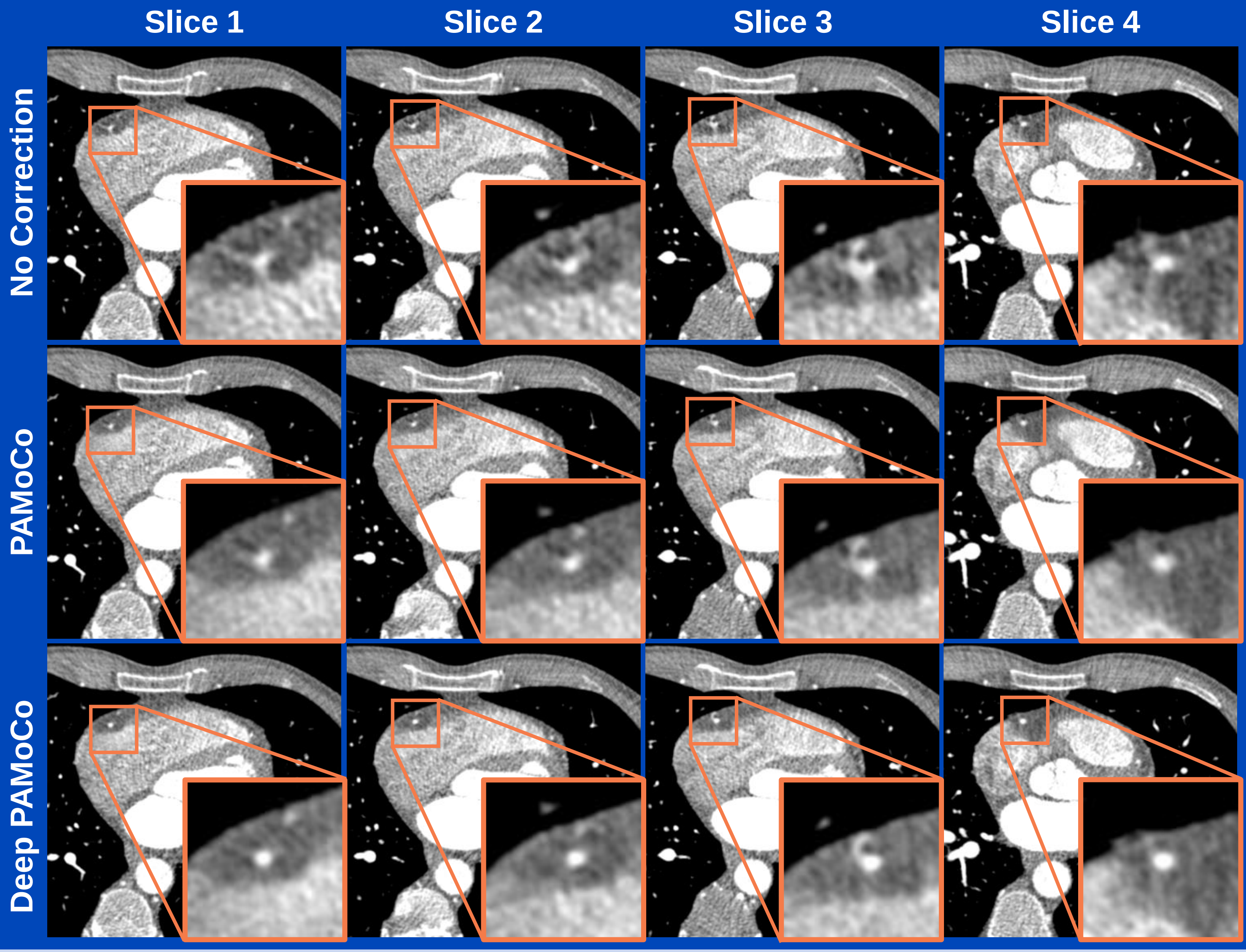

C = 1000 HU
W = 1000 HU

J. Maier, S. Lebedev, E. Eulig, S. Sawall, E. Fournié, K. Stierstorfer, and M. Kachelrieß. Coronary artery motion compensation for short-scan cardiac CT using a spatial transformer network. Conference Program of the 6th International CT-Meeting, August 2020.

Results

Measurements, patient 3

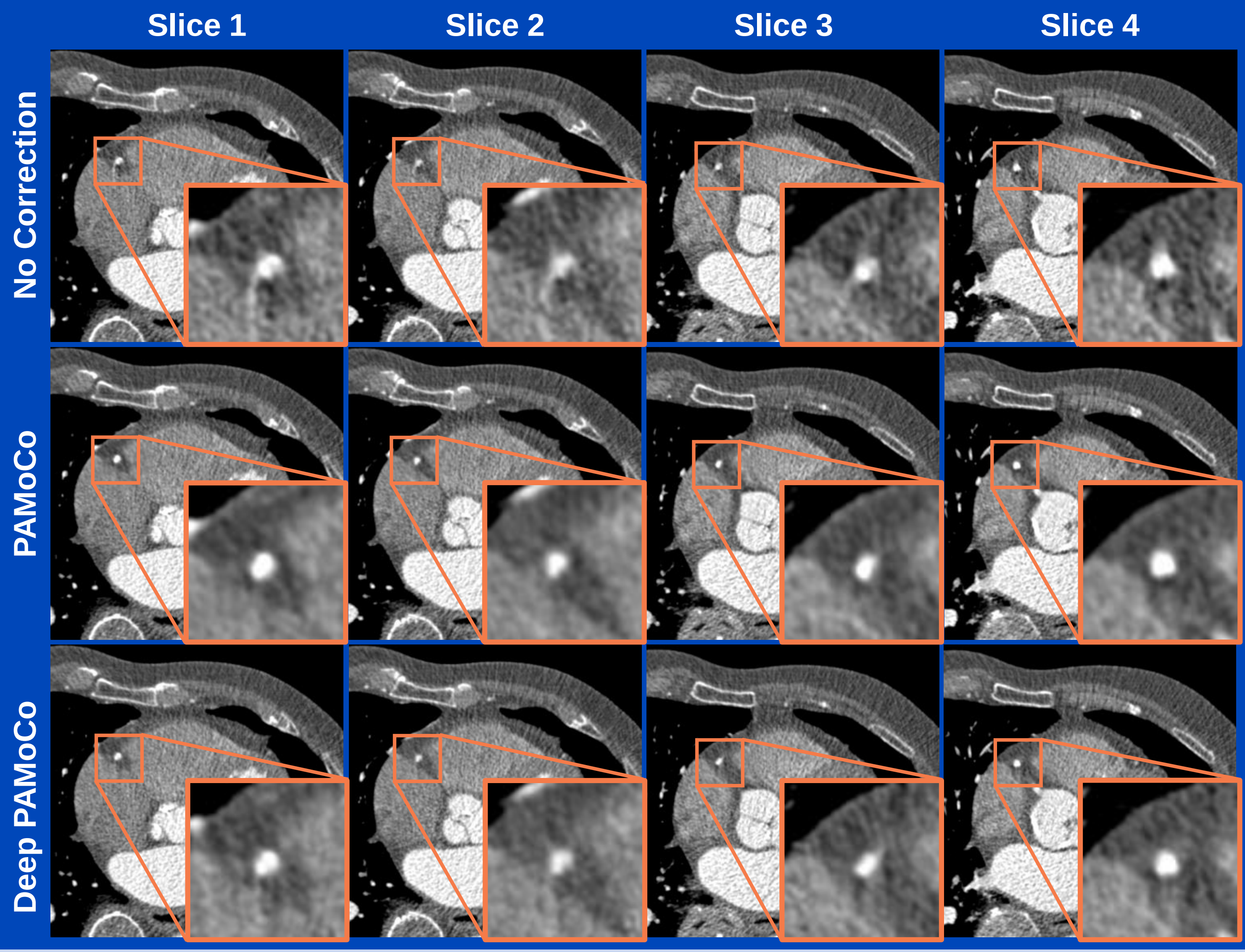

C = 1100 HU
W = 1000 HU

J. Maier, S. Lebedev, E. Eulig, S. Sawall, E. Fournié, K. Stierstorfer, and M. Kachelrieß. Coronary artery motion compensation for short-scan cardiac CT using a spatial transformer network. Conference Program of the 6th International CT-Meeting, August 2020.

4D CBCT MoCo with Deep Image Registration?

- 4D CBCT refers to respiratory-gated CBCT images
- Due to gating, streak artifacts typically occur
- A motion compensation (MoCo) helps to warp the respiratory phases into a target phase. MoCo requires to estimate the motion vector fields (MVFs).
- MVF estimation uses deformable registration.

Examples for CBCT MoCo

3D CBCT Standard	4D gated CBCT Conventional Phase-Correlated	sMoCo Standard Motion Compensation	acMoCo Artifact Model-Based Motion Compensation

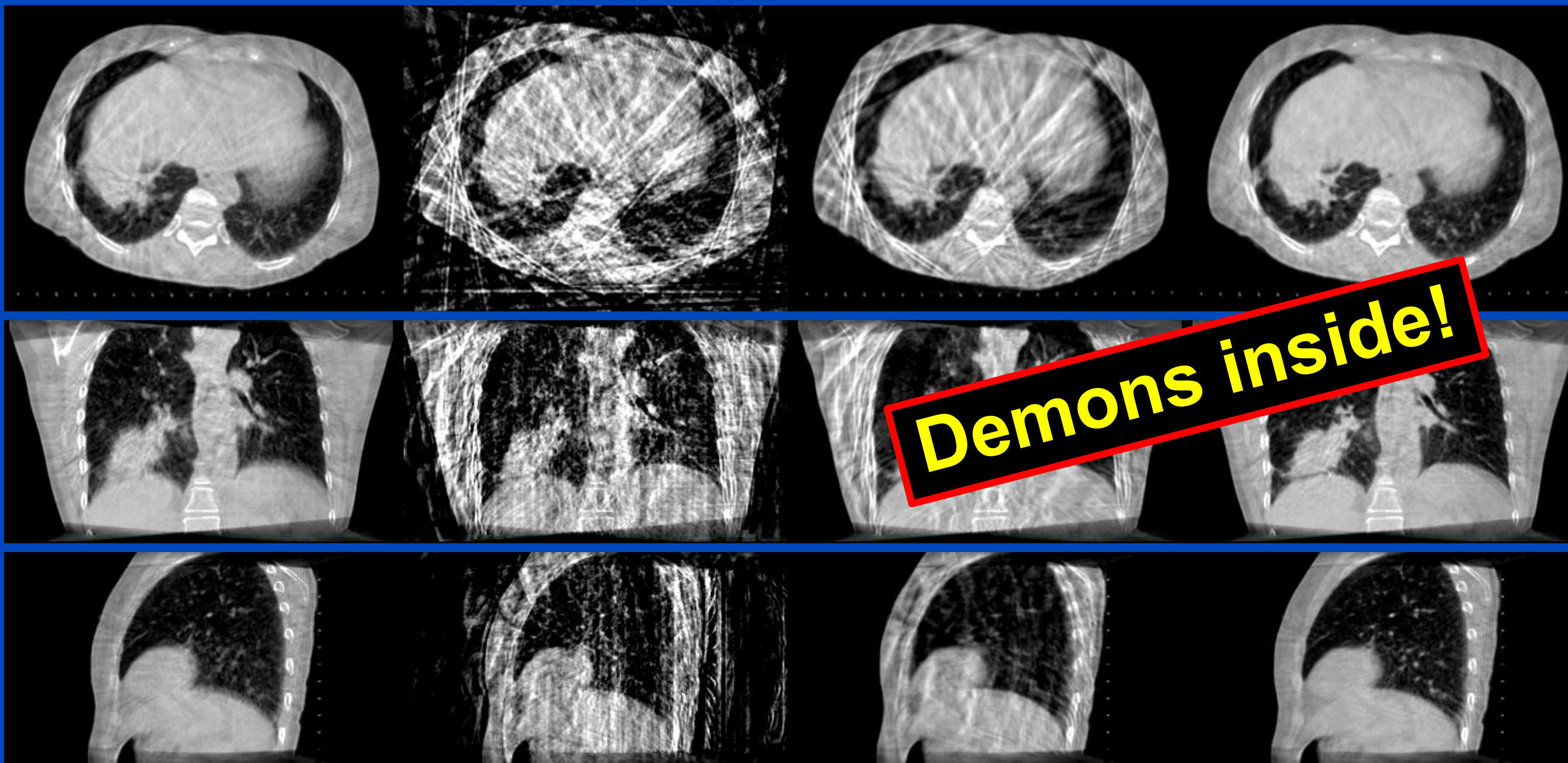

sMoCo: Li, Koong, and Xing, “Enhanced 4D cone–beam CT with inter–phase motion model,” Med. Phys. 51(9), 3688–3695, 2007.
cMoCo: Brehm, Paysan, Oelhafen, Kunz, and Kachelrieß, “Self-adapting cyclic registration for motion-compensated cone-beam CT in image-guided radiation therapy,” Med. Phys. 39(12):7603-7618, 2012.
acMoCo: Brehm, Paysan, Oelhafen, and Kachelrieß, “Artifact-resistant motion estimation with a patient-specific artifact model for motion-compensated cone-beam CT” Med. Phys. 40(10):101913, 2013.

varian

1 min shifted detector CBCT scan with about 12 respiratory cycles, displayed with 30 rpm.
Patient data provided by Memorial Sloan–Kettering Cancer Center, New York, NY. C = -200 HU, W = 1400 HU

dkfz.

Demons Deformable Registration

- Static target image s
- Model to be deformed m
- Find transformation vector field T, i.e. $s = m \circ \mathrm{T}$
- Demons algorithm
  - Displacement update u by intensity matching on linear approximation

$$\boldsymbol{u} = \frac{m - s}{\|\boldsymbol{\nabla} s\|^2 + (m - s)^2} \boldsymbol{\nabla} s$$

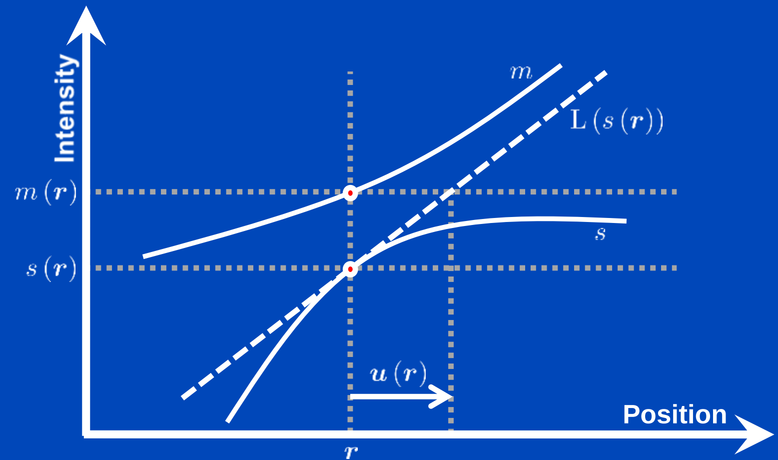

- Regularization
  - Two Gaussian convolution kernels $G_{\text{fluid}}, G_{\text{diffusion}}$

$$\mathrm{T} \leftarrow G_{\text{diffusion}} * (\mathrm{T} \circ \exp(G_{\text{fluid}} * \boldsymbol{u}))$$


Target


Model

Deformed model matching target

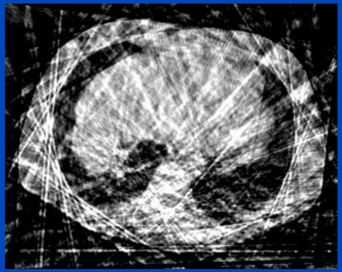

Thirion, "Image matching as a diffusion process: An analogy with Maxwell's demons," Medical Image Analysis 2(3), 243–260, 1998.

VoxelMorph Deformable Registration

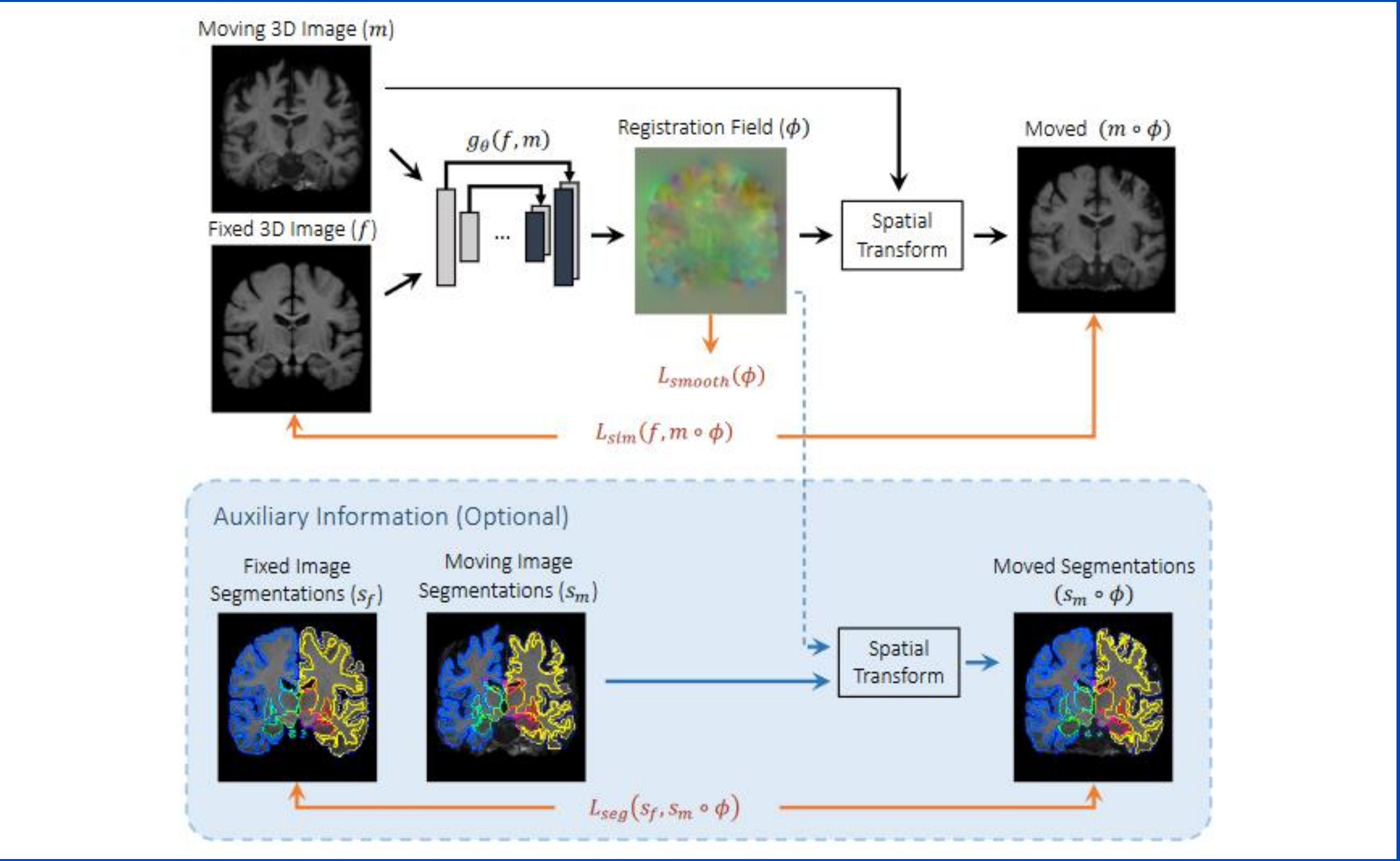

Balakrishnan, G., Zhao, A., Sabuncu, M. R., Guttag, J. and Dalca, A. V., "VoxelMorph: A Learning Framework for Deformable Medical Image Registration," IEEE Trans. Med. Imaging 38(8), 1788–1800, 2019.

dkfz.

Demons vs. VoxelMorph

- Cost/loss functions of Demons and VoxelMorph are identical if we use the L_2-norm for the vector field regularization and the MSE for the image similarity

$$C = \arg\min_{\phi} \left\| m(\phi) - f \right\|_2^2 + \lambda \left\| \nabla \phi \right\|_2^2$$

- Demon's hierarchical registration cascade corresponds to VoxelMorph's hierarchical encoder/decoder stages.
- Both methods can be extended to estimate a diffeomorphic vector field, i.e. a differentiable and invertible vector field.
- Demons minimizes the cost function for every patient, while VoxelMorph learned to minimize it for the training parients and then applies its knowledge to other patients.
- Demons may be slower than VoxelMorph (a thorough comparison is missing), but is certainly more reliable and predictable.

Deep MoCo

4D FDK	deep sMoCo (VoxelMorph)	deep cMoCo (VoxelMorph)	deep acMoCo (VoxelMorph)	acMoCo (Demons)

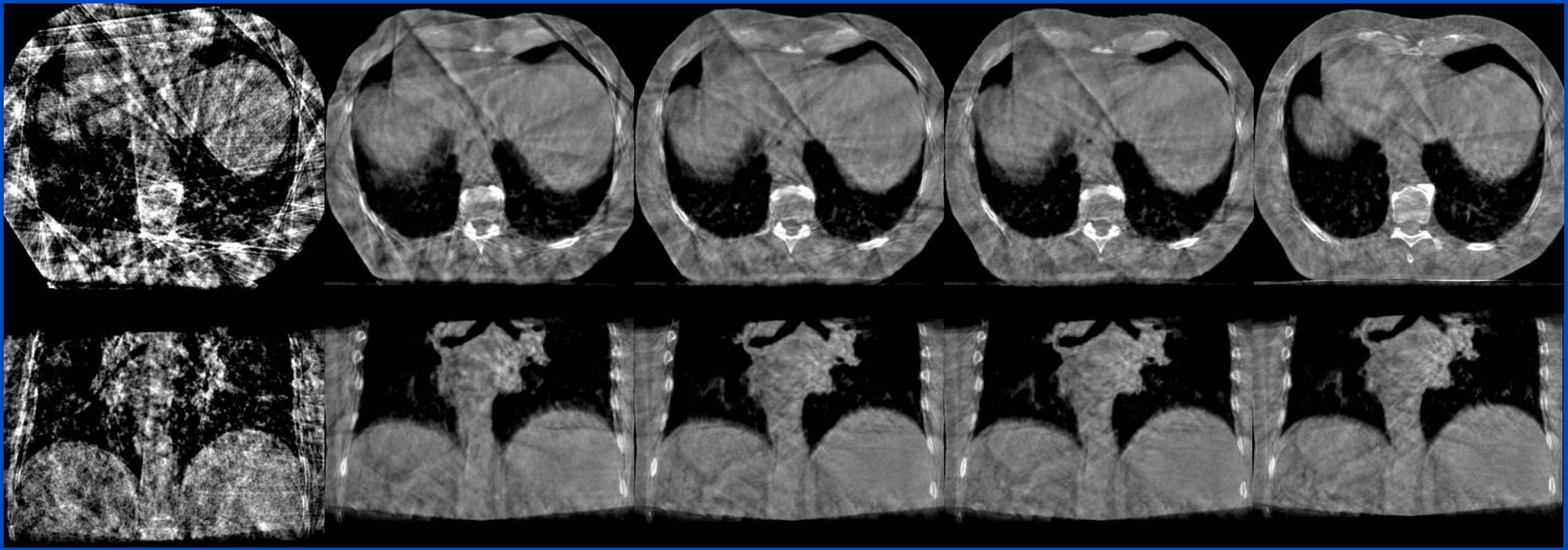

			Faster computation	Less artifacts

Intervention goes Deep!

Deep DSA

???

Without mask?

Methods
General principle

Conventional DSA

I_t $-$ I_0 $=$ $\tilde{I}_t$

Deep DSA

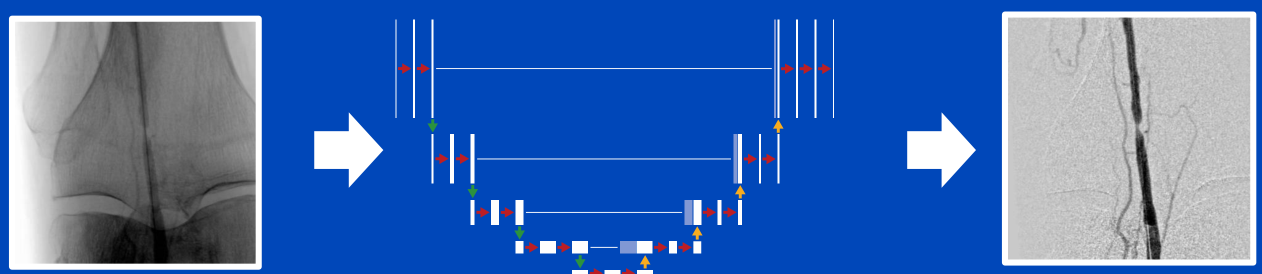

I_t $\tilde{I}_t$

- **Train on static cases where ground truth is conventional DSA**

E. Eulig, M. Kachelrieß, et al. "Learned digital subtraction angiography (Deep DSA): method and application to lower extremities". Proc. SPIE 11072, 15th International Meeting on Fully Three-Dimensional Image Reconstruction, 1107223:1-4, May 2019.

Methods

General principle

Conventional DSA

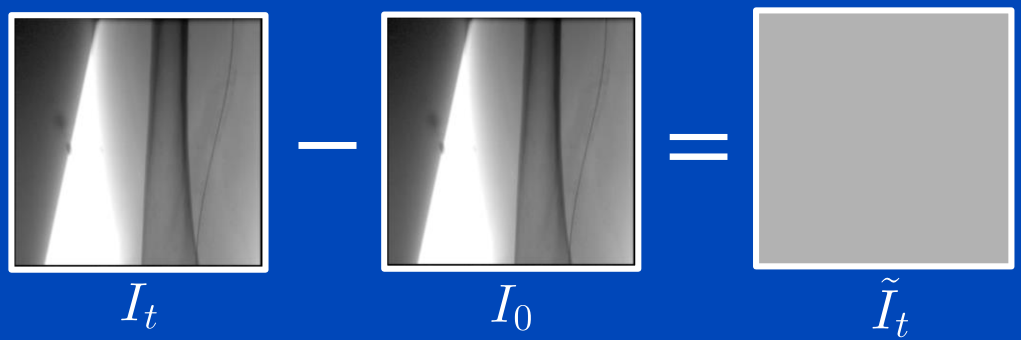

Deep DSA

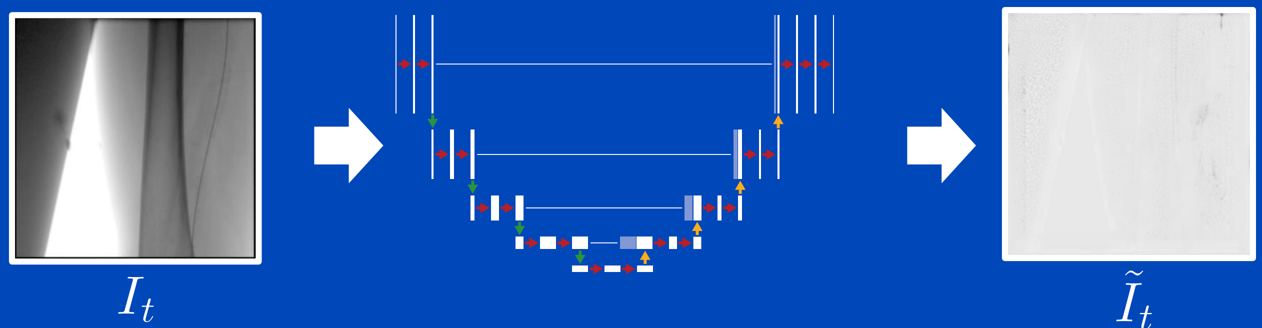

- **Train on static cases where ground truth is conventional DSA**
- **During inference CNN can be applied to both static and dynamic cases**

E. Eulig, M. Kachelrieß, et al. "Learned digital subtraction angiography (Deep DSA): method and application to lower extremities". Proc. SPIE 11072, 15th International Meeting on Fully Three-Dimensional Image Reconstruction, 1107223:1-4, May 2019.

Results

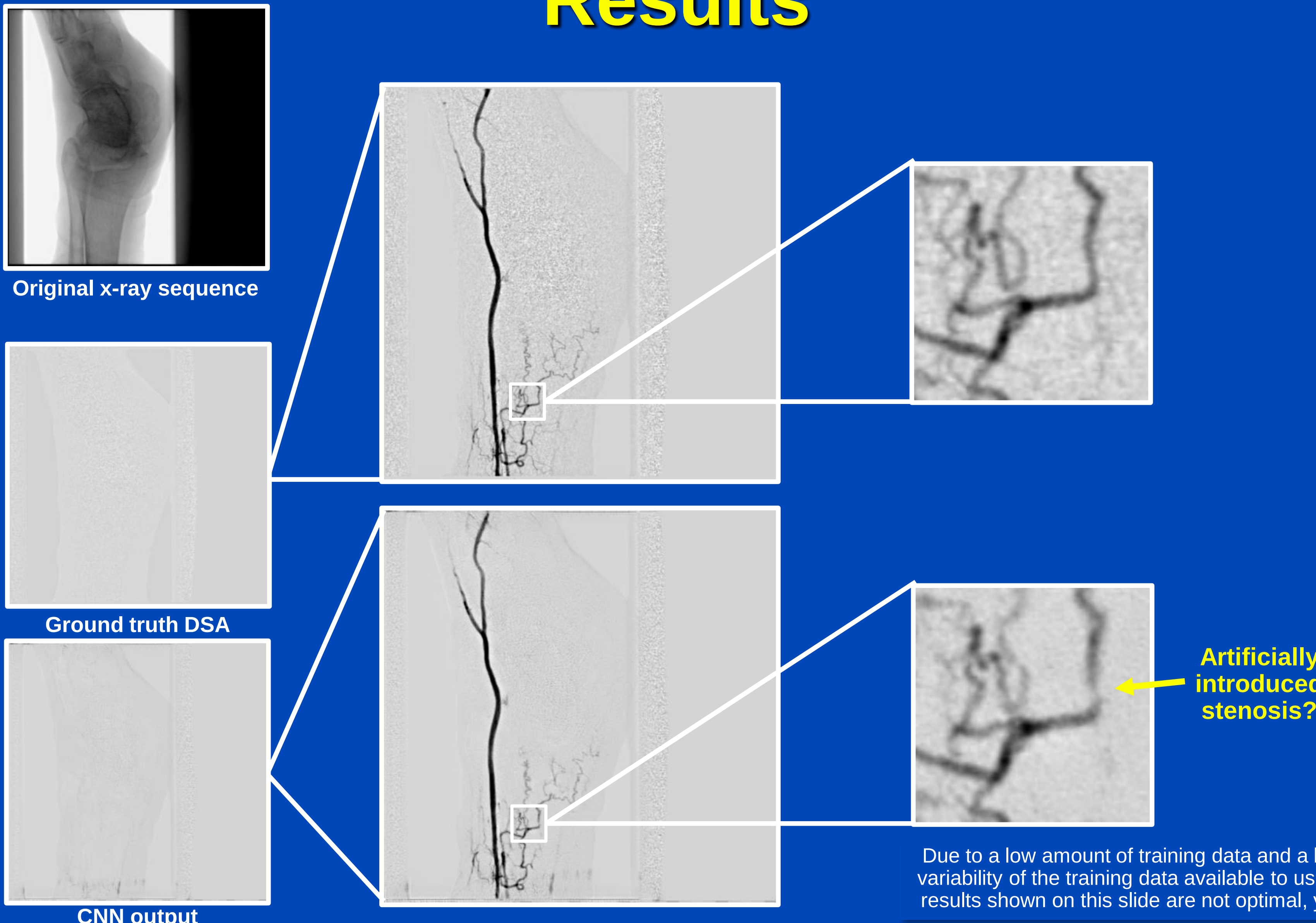

Due to a low amount of training data and a low variability of the training data available to us the results shown on this slide are not optimal, yet.

E. Eulig, M. Kachelrieß, et al. "Learned digital subtraction angiography (Deep DSA): method and application to lower extremities". Proc. SPIE 11072, 15th International Meeting on Fully Three-Dimensional Image Reconstruction, 1107223:1-4, May 2019.

Deep DSA

Fluoroscopy

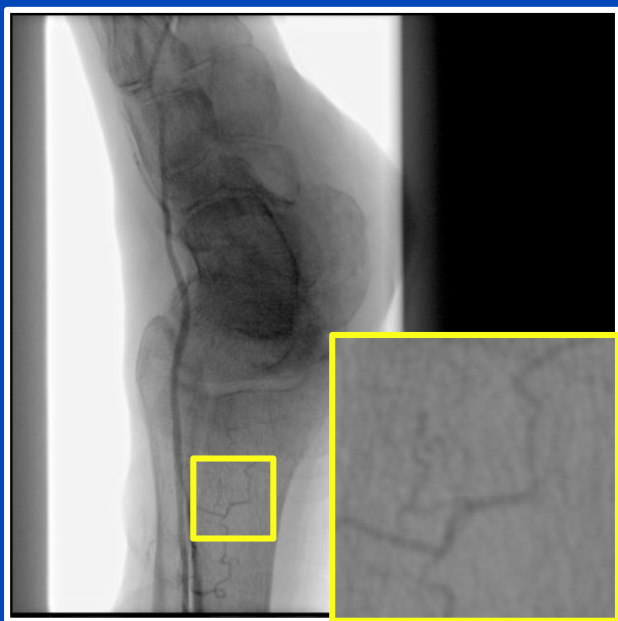

DSA (fluoro minus mask)

Deep DSA (from fluoro only)

Due to a low amount of training data and a low variability of the training data available to us the results shown on this slide are not optimal, yet.

E. Eulig, M. Kachelrieß, et al. "Learned digital subtraction angiography (Deep DSA): method and application to lower extremities". Proc. SPIE 11072, 15th International Meeting on Fully Three-Dimensional Image Reconstruction, 1107223:1-4, May 2019.

Results

Bolus chase study

Dynamic fluoroscopy

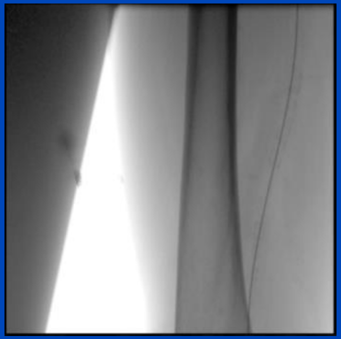

Conventional DSA

Conventional DSA infeasible due to C-arm motion

Deep DSA

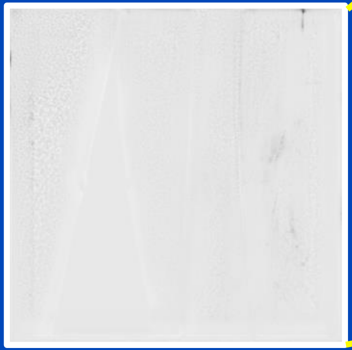

Deep DSA at t $= t_a$

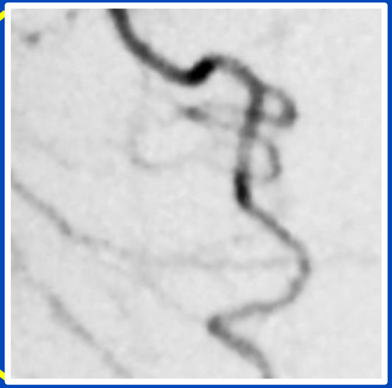

Deep DSA at t $= t_a$

E. Eulig, M. Kachelrieß, et al. "Learned digital subtraction angiography (Deep DSA): method and application to lower extremities". Proc. SPIE 11072, 15th International Meeting on Fully Three-Dimensional Image Reconstruction, 1107223:1-4, May 2019.

Deep 3D+T Fluoroscopy

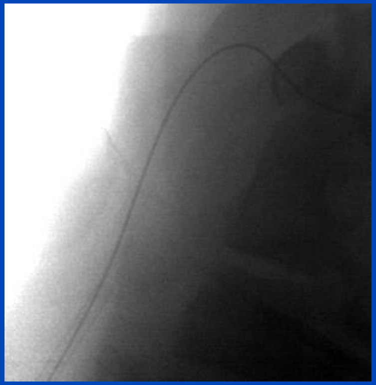

???

At 2D+T dose?

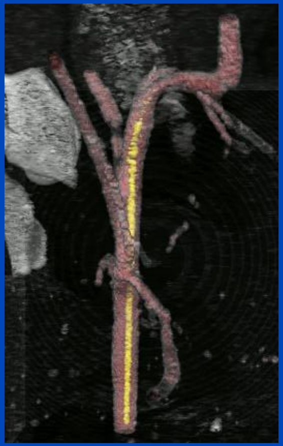

Deep 3D+T Tomographic Fluoroscopy

either 2D+T fluoroscopy

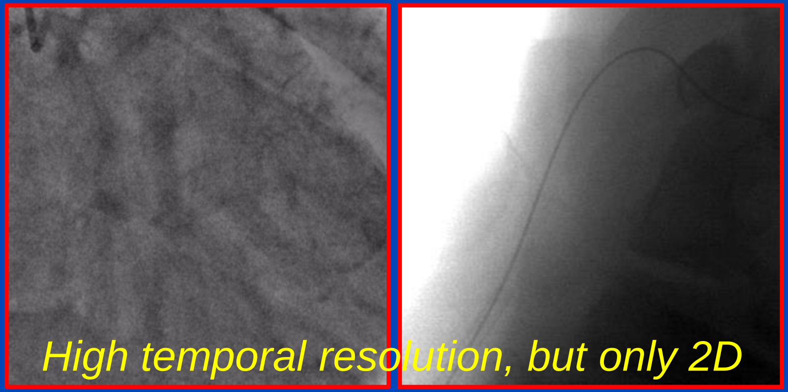

or 3D tomography

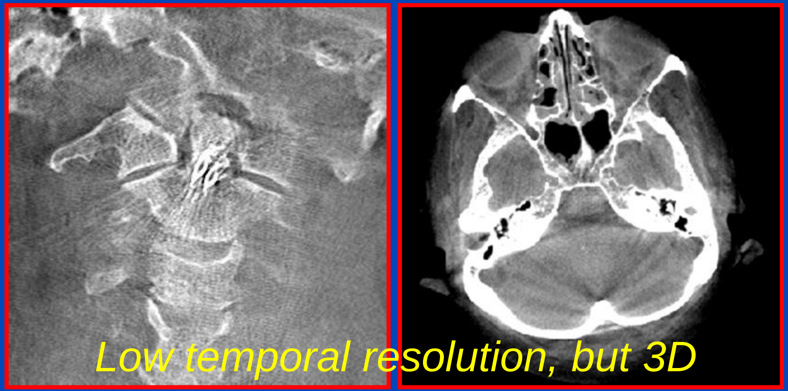

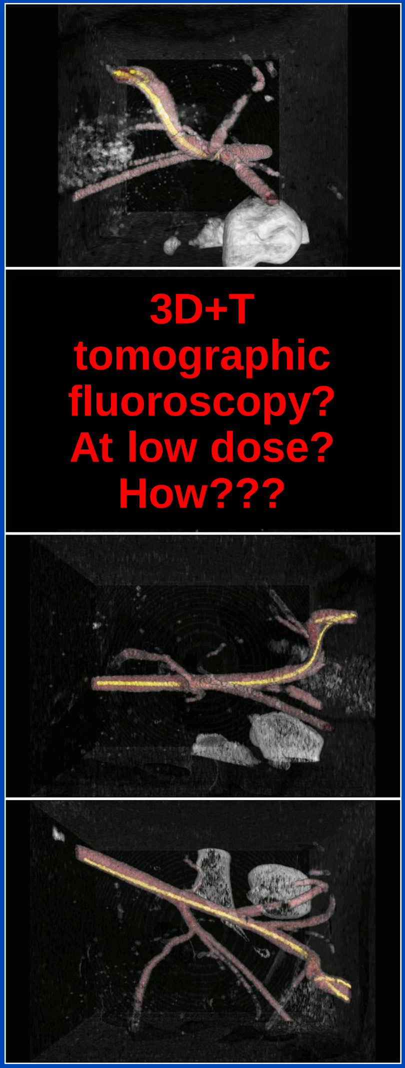

How to Realize 3D+T Fluoroscopy

- Low dose by:
  - Low tube current
  - Very few projections (pulsed mode)
- Advantages of intervention guidance:
  - Repetitive scanning of the same body region: changes are sparse.
  - Interventional materials are fine structures (few voxels) of high contrast (metal).

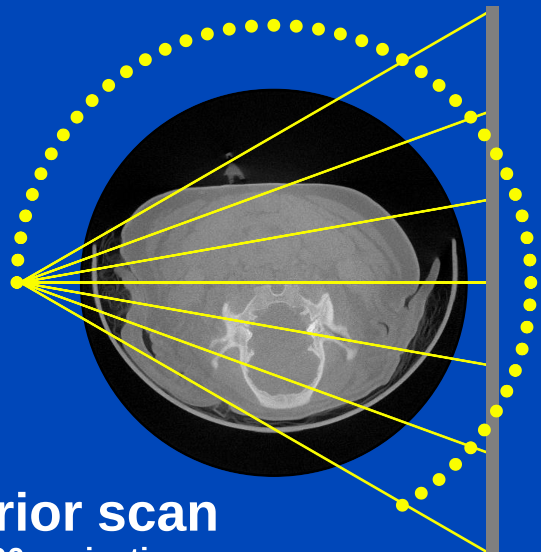

Prior scan
400 projections

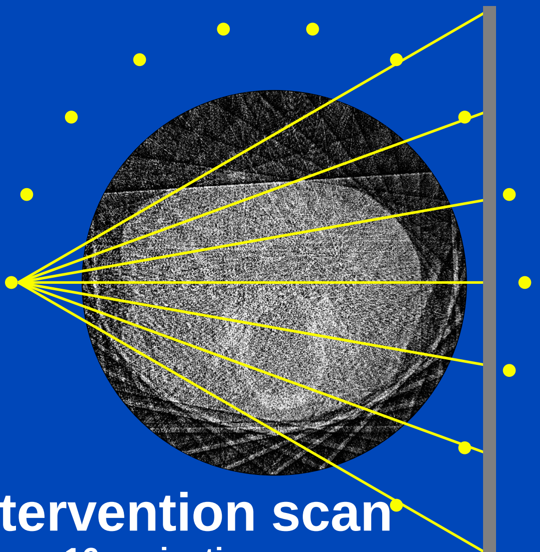

Intervention scan
16 projections

Experimental setup

B. Flach, J. Kuntz, M. Brehm, R. Kueres, S. Bartling, and M. Kachelrieß. "Low dose tomographic fluoroscopy: 4D intervention guidance with running prior.", Med. Phys. 40:101909, 11 pages, October 2013.

3D+T Image Guidance at 2D+T Dose

Stent Expansion in the Carotis of a Pig with Angio Roadmap Overlay

Iterative reconstruction using prior knowledge inside!

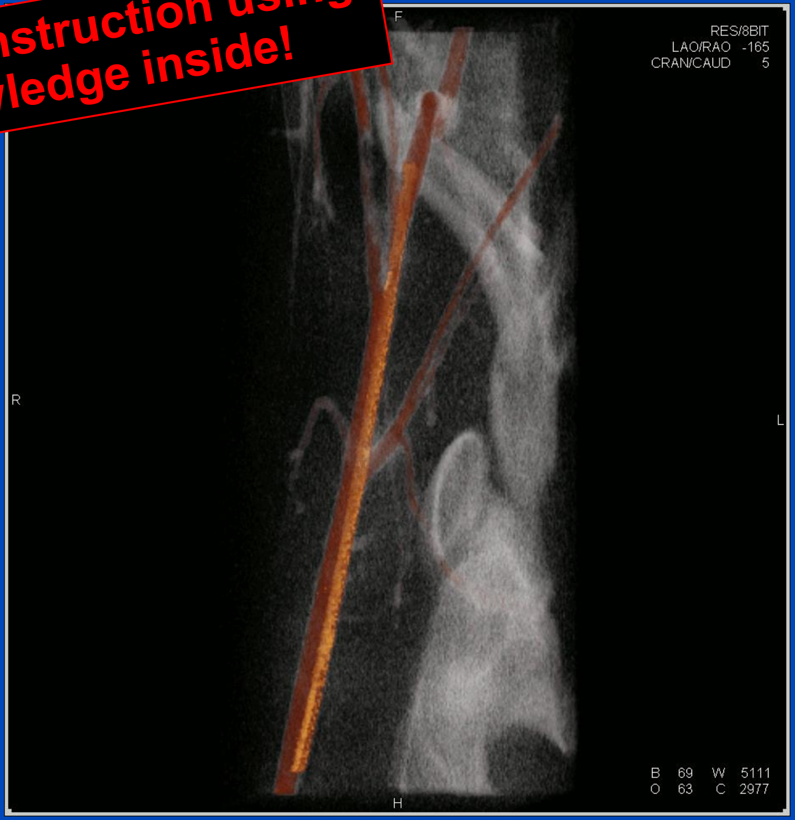

Dose of the yet unoptimized approach: 20 bis 50 µGy/s.

This work was awarded the intervention award 2013 of the German Society of Neuroradiology (DGNR).
This work was further selected as the Editor's Pick for the Medical Physics Scitation site.

3D+T Fluoroscopy at 2D+T Dose

Guide Wire in the Carotis of a Pig with Angio Roadmap Overlay

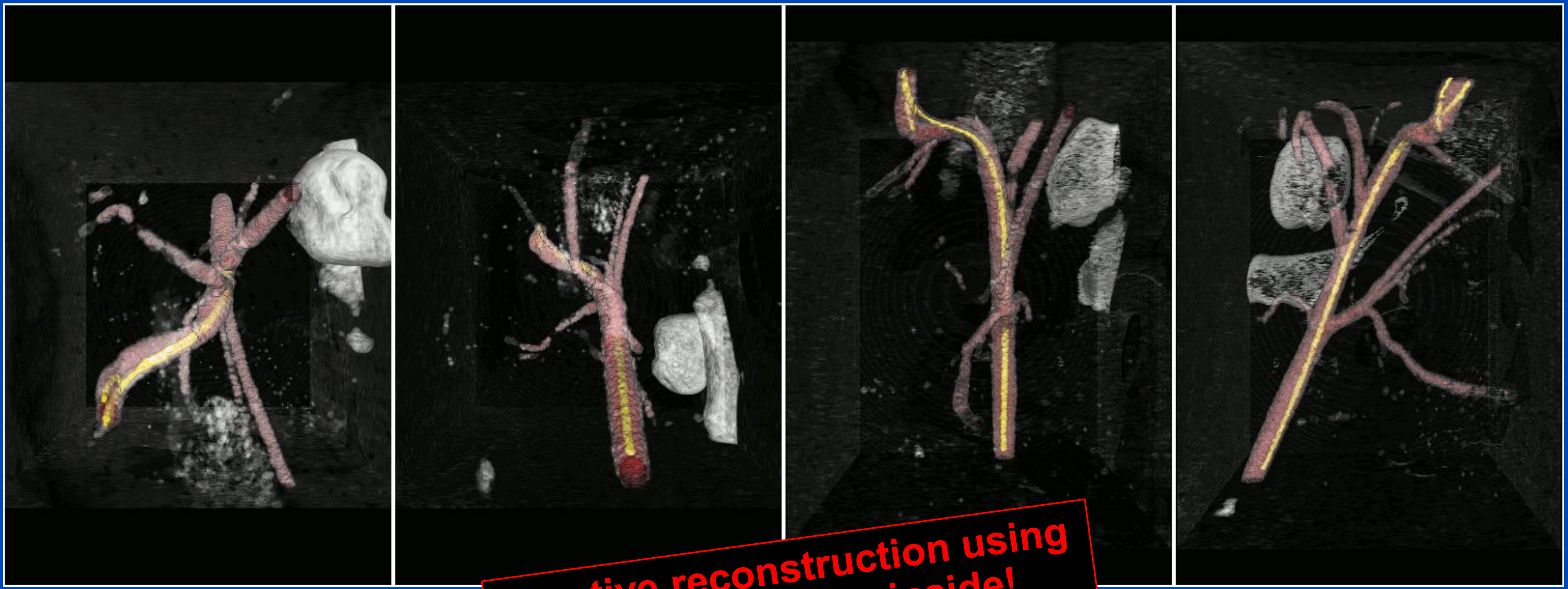

Iterative reconstruction using prior knowledge inside!

Dose of the yet unoptimized approach: 20 to 50 µGy/s. Obviously, 16 projections are too much.

This work was awarded the intervention award 2013 of the German Society of Neuroradiology (DGNR).
This work was further selected as the Editor's Pick for the Medical Physics Scitation site.

Method

Deep Tool Extraction (DTE), Feldkamp Recon (FDK), Deep Tool Reconstruction (DTR)

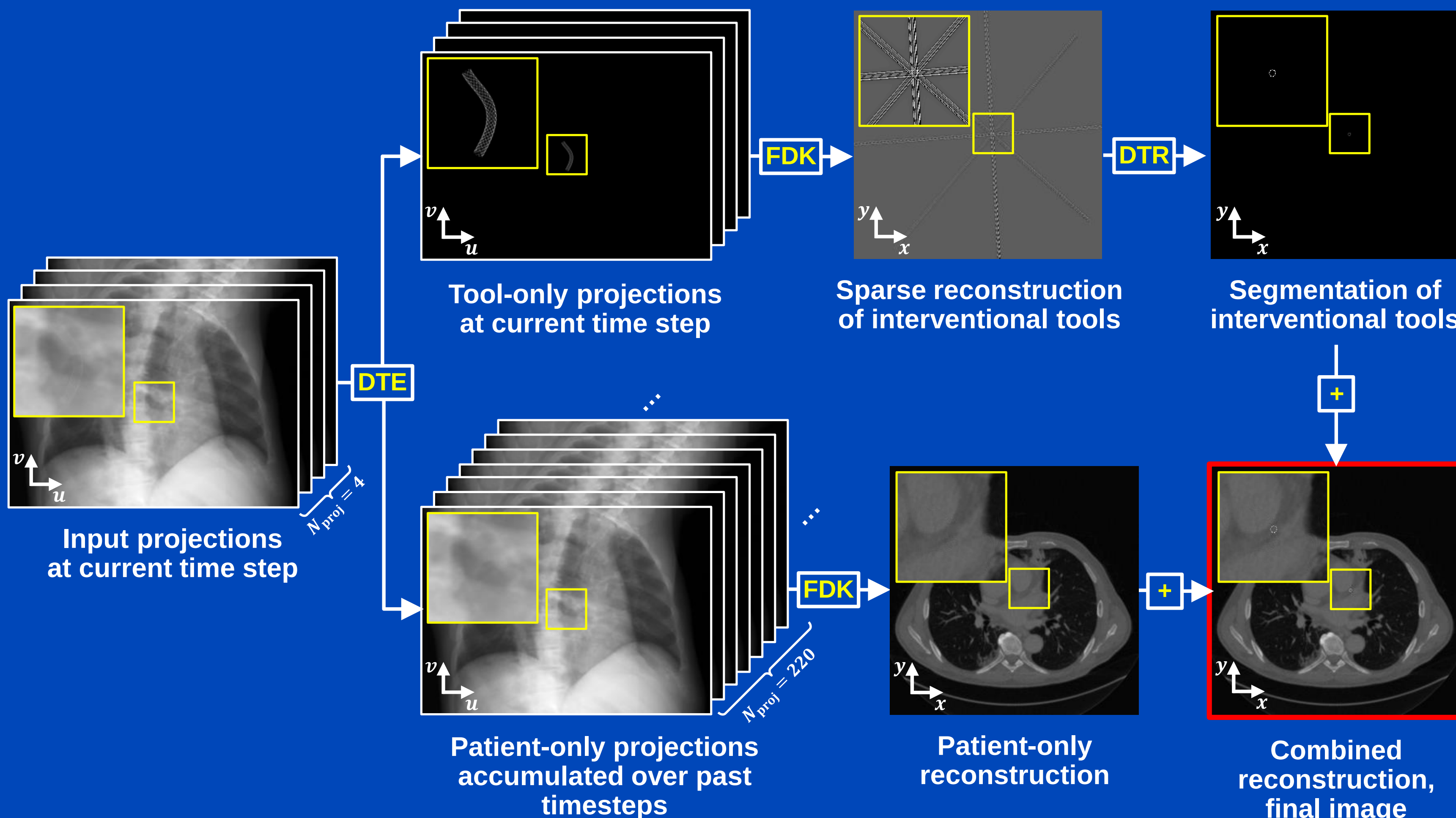

E. Eulig, J. Maier, N.R. Bennet, M. Knaup, K. Hörndler, A. Wang, and M. Kachelrieß. Deep learning-aided CBCT image reconstruction of interventional material from four x-ray projections. SPIE Medical Imaging Conference Record, 113121L:1-7, March 2020.

Zeego @ Stanford University

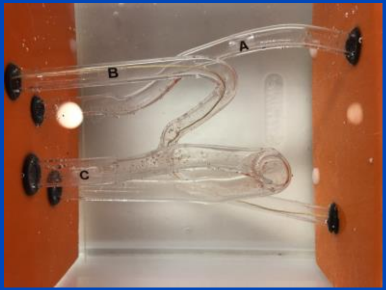

dkfz.

Zeego Measurements with Just 4 Projections

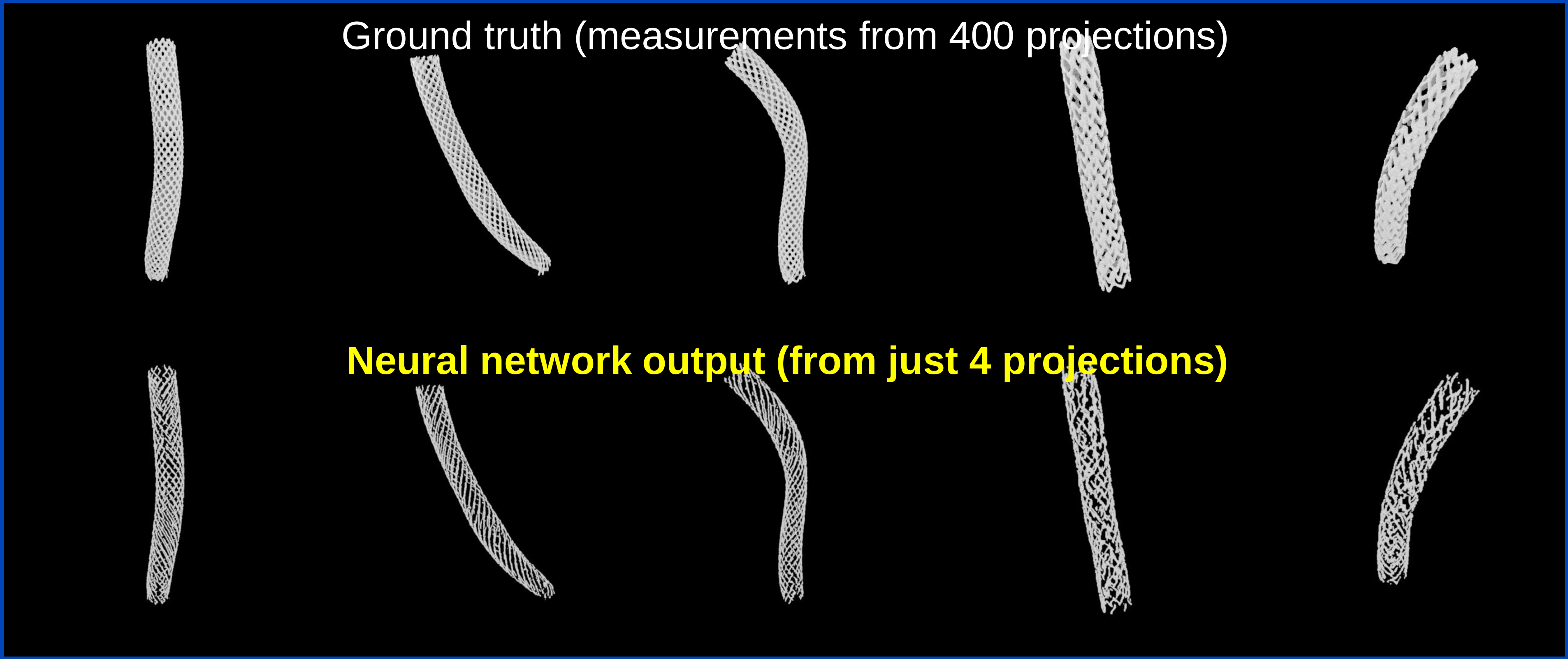

Loop through slices reconstructed from just 4 projections without AI:

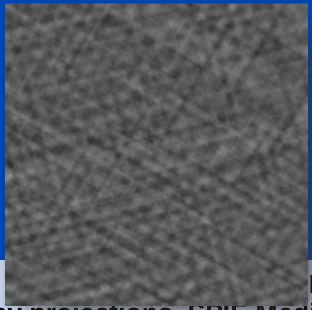

Stent examples:

E. Eulig, J. Maier, N.R. Bennet, M. Knaup, K. … M. Kachelrieß. Deep l… of interventional material from four x-ray projections. SPIE Medical Imaging Conference Record, 113121L:1-7, March 2020.

Thank You!

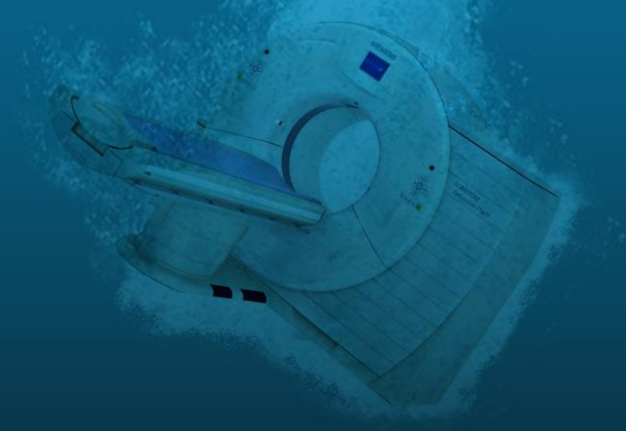

This presentation is available at www.dkfz.de/ct.

Job opportunities through DKFZ’s international PhD or Postdoctoral Fellowship programs (marc.kachelriess@dkfz.de).

Parts of the reconstruction software were provided by RayConStruct® GmbH, Nürnberg, Germany.